AD_____
(Leave blank)

Award Number: W81XWH-07-1-0523

TITLE: Biochemical characterisation of *TSC1* and *TSC2* variants identified in patients with tuberous sclerosis complex

PRINCIPAL INVESTIGATOR: Mark Nellist

CONTRACTING ORGANIZATION: Erasmus MC
The Netherlands

REPORT DATE: July 2009

TYPE OF REPORT: Annual

PREPARED FOR: U.S. Army Medical Research and Materiel Command
Fort Detrick, Maryland 21702-5012

DISTRIBUTION STATEMENT: (Check one)

X Approved for public release; distribution unlimited

☐ Distribution limited to U.S. Government agencies only;
report contains proprietary information

# REPORT DOCUMENTATION PAGE

*Form Approved*
*OMB No. 0704-0188*



| 1. REPORT DATE | 2. REPORT TYPE | 3. DATES COVERED |
|---|---|---|
| (31-07-2009) | Annual | 1 Jul 2008 - 30 Jun 2009 |

**4. TITLE AND SUBTITLE**
Biochemical characterisation of TSC1 and TSC2 variants identified in patients with tuberous sclerosis complex

**5a. CONTRACT NUMBER**
W81XWH-07-1-0523

**5b. GRANT NUMBER**

**5c. PROGRAM ELEMENT NUMBER**

**6. AUTHOR(S)**

Mark Nellist

Email: m.nellist@erasmusmc.nl

**5d. PROJECT NUMBER**

**5e. TASK NUMBER**

**5f. WORK UNIT NUMBER**

**7. PERFORMING ORGANIZATION NAME(S) AND ADDRESS(ES)**

Erasmus MC
The Netherlands

**8. PERFORMING ORGANIZATION REPORT NUMBER**

**9. SPONSORING / MONITORING AGENCY NAME(S) AND ADDRESS(ES)**
U.S. Army Medical Research and Materiel Command
Fort Detrick, Maryland 21702-5012

**10. SPONSOR/MONITOR'S ACRONYM(S)**

**11. SPONSOR/MONITOR'S REPORT NUMBER(S)**

**12. DISTRIBUTION / AVAILABILITY STATEMENT**
Approved for Public Release; Distribution Unlimited

**13. SUPPLEMENTARY NOTES**

**14. ABSTRACT**

The key findings of the project during the research period (23/1/09 - 31/7/09) are as follows: 1. Derivation and testing of 31 unclassified TSC2 variants: 16 classified as pathogenic; 7 classified as neutral; 8 still unclassified/analysis not complete. 2. Derivation of 12 unclassified TSC1 variants: 3 classified as pathogenic; 7 classified as neutral; 2 still unclassified/analysis not complete. 3. Improved assay cost, throughput and reproducibility. 4. Idenbtification of variants with an intermediate effect on TSC1-TSC2 activity.

**15. SUBJECT TERMS**

Tuberous Sclerosis Complex, unclassified variants, TSC1, TSC2

| 16. SECURITY CLASSIFICATION OF: | | | 17. LIMITATION OF ABSTRACT | 18. NUMBER OF PAGES | 19a. NAME OF RESPONSIBLE PERSON |
|---|---|---|---|---|---|
| a. REPORT | b. ABSTRACT | c. THIS PAGE | | | USAMRMC |
| U | U | U | UU | 74 | 19b. TELEPHONE NUMBER *(include area code)* |

**Standard Form 298 (Rev. 8-98)**
**Prescribed by ANSI Std. Z39.18**

## Table of Contents

## Introduction

*Subject*: Tuberous sclerosis complex (TSC) is a genetic disorder affecting approximately 1 in 10 000 individuals (1). TSC is caused by mutations in either the *TSC1* or *TSC2* tumour suppressor genes (2, 3). The *TSC1* and *TSC2* gene products form a protein complex that inhibits the activity of the mammalian target of rapamycin (mTOR) complex 1 (TORC1). TORC1 coordinates nutritional, hormonal and other cues to regulate the cellular growth machinery. Therefore, inactivation of the TSC1-TSC2 complex results in inappropriate TORC1 activity and cell growth defects (4).

Mutation analysis of the *TSC1* and *TSC2* genes is a useful diagnostic tool for helping individuals and families affected by TSC (5). In most cases of TSC, a definite pathogenic *TSC1* or *TSC2* mutation is identified. However, in some cases it is difficult to determine whether sequence changes identified in the *TSC1* or *TSC2* genes are pathogenic, or not. These 'unclassified variants', typically missense changes, small in-frame insertions or deletions, or changes that could affect splicing, present a significant problem for diagnostics and genetic counselling.

*Purpose*: The purpose of this research project is to develop and apply assays of TSC1-TSC2 function to determine whether specific unclassified *TSC1* and *TSC2* variants are pathogenic or not. In this way, the individuals carrying these variants, as well as their families, can obtain clearer information about their condition and the associated risks. Furthermore, correlation of the biochemical effects of the different variants with the observed patient phenotypes could provide insight into genotype-phenotype correlations in TSC, and identification of amino acids and/or regions that are important for different aspects of TSC1-TSC2 function could help define the structural and catalytic domains of the TSC1-TSC2 complex.

*Scope*: The specific aims of the project are to:

1. Apply functional assays to determine whether specific *TSC1* and *TSC2* variants are pathogenic mutations.
2. Determine whether specific *TSC1* and *TSC2* mutations are associated with specific TSC phenotypes.
3. To identify amino acid residues that are essential for TSC1 or TSC2 function.
4. To develop a simple, reliable and rapid test for TSC1-TSC2 function.

**Body**

*1. Application of functional assays to determine whether specific TSC1 and TSC2 variants are pathogenic mutations.*

The TSC1-TSC2 complex inhibits the mammalian target of rapamycin (mTOR) complex 1 (TORC1), preventing the phosphorylation of TORC1 substrates, including p70 S6 kinase (S6K) (4). To investigate the effects of amino acid substitutions and small in-frame insertions or deletions on TSC1 and TSC2 function, we introduced the corresponding nucleotide changes into *TSC1* and *TSC2* expression constructs by site-directed mutagenesis and expressed the variant proteins in mammalian cells in culture. After 24 hours, cell lysates were prepared and subjected to denaturing polyacrylamide gel electrophoresis (SDS-PAGE). After transfer to nitrocellulose membranes, the activity of the TSC1 and TSC2 variants was estimated by immunoblotting. The phosphorylation status of ectopically expressed p70 S6 kinase and the expression levels of the TSC1 and TSC2 variants were determined using an Odyssey infra-red scanner (Li-Cor Biosciences). Phosphorylated S6K was detected using a commercially available antibody specific for phosphorylation at the T389 position (1A5, Cell Signaling Technology); TSC1 and total S6K were detected with a rabbit polyclonal antibody against the myc epitope tag (Cell Signaling Technology); TSC2 was detected with a rabbit polyclonal antibody (6). Unclassified *TSC1* and *TSC2* variants were selected from our patient cohort (5), from the Leiden Open Variation Database (7, 8), from published TSC case reports (9), or through specific requests from genetic counsellors.

In the last 6 month period (23/1/09 - 31/7/09) we have analysed 31 TSC2 variants and 12 TSC1 variants (see Supporting Data; Part 1, Tables 1 and 2). In addition, for 67 previously characterised TSC2 variants, we applied systematic criteria to determine whether TSC1-TSC2 function is affected by the corresponding amino acid changes (Supporting Data; Part 1, Table 2).

A revised manuscript describing the analysis of 12 TSC1 variants has been submitted for publication (Supporting Data; Part 2), and the analysis of additional TSC1 and TSC2 variants has been completed (Supporting Data; Part 3, Figures 1 and 2, respectively). Furthermore, we have assayed the effects of a number of truncating *TSC1* mutations on the activity of the TSC1-TSC2 complex. The results of these experiments are shown in Supporting Data, Part 3, Figure 3. Deletion of TSC1 amino acids 901 - 1164, 693 - 1164 or 1 -350 did not completely inactivate the TSC1-TSC2 complex,

indicating that both the the N- and C-terminal regions of TSC1 are involved in maintaining the activity of the TSC1-TSC2 complex. Deletion of the N-terminal amino acids 1 -350 had a similar effect on TSC1 function as the pathogenic missense changes identified within this region (Supporting Data; Part 2 and Part 3).

Some substitutions had no discernible effect on the activity of the TSC1-TSC2 complex in our assays. We concluded that these were neutral variants, and not responsible for the TSC phenotype, unless there was evidence from predictive computer-based algorithms that the nucleotide changes could affect splicing (10 - 12). We have now obtained ethical approval to approach patients for skin biopsies. Therefore, we can now seek actual evidence of aberrent splicing in RNA isolated from fibroblasts from patients carrying these putative splice mutations using reverse transcriptase-polymerase chain reaction (RT-PCR), in combination with DNA sequencing.

So far, we have identified 8 reported missense changes (3 in *TSC2* and 5 in *TSC1*) that do not affect TSC1 or TSC2 function, but according to the splice site prediction programs, may be splice site mutations (Supporting Data; Part 1, Tables 1 and 2). We have already been able to analyse mRNA from a patient with a *TSC2* c.1235A>T nucleotide change (Supporting Data; Part 1, Table 2, and Part 3, Figures 4 and 5). First, fibroblasts from the patient were obtained in culture. To inhibit nonsense-mediated RNA decay, and thereby increase the rate of detection of aberrantly spliced mRNAs, the cells were treated with cycloheximide. RNA was prepared from the fibroblast culture and RT-PCR was performed. A novel splice isoform was detected that resulted in a small in-frame deletion of 8 amino acids (TSC2 412del8). This isoform was not detected in RNA isolated from control individuals. The TSC2 412del8 change was tested using the functional assays described above. The 412del8 had a significant effect on TSC2 function (Supporting Data; Part 3, Figure 5) and we concluded that the *TSC2* c.1235A>T mutation was a pathogenic splice site mutation.

*2. Determine whether specific TSC1 and TSC2 mutations are associated with specific TSC phenotypes.*

Functional studies can help establish whether specific changes in the *TSC1* and *TSC2* genes are pathogenic. Interestingly, some variants identified in individuals and/or families exhibiting only mild or minor symptoms of TSC appear to have intermediate activity in our functional assays (13). We classified the different TSC2 variants

according to the results of the immunoblot assay and have consequently identified several variants that may have an intermediate effect on TSC1-TSC2 function (Supporting Data; Part 1, Table 2 and Part 3, Figure 3). We are currently investigating in more detail how these changes affect the TSC1-TSC2 complex, and whether there is an association between these variants and patients with a less severe TSC phenotype. Our *in vitro* observations of human TSC1 and TSC2 variants with intermediate activity are consistent with a recent report of a mouse model of TSC with a less severe phenotype (14).

*3. Identification of amino acid residues/domains that are essential for TSC1 or TSC2 function.*

Amino acid substitution prediction methods use sequence and/or structural information to predict the effects of amino acid changes on protein function (15, 16). In the absence of adequate genetic or functional data, prediction methods have been applied to try and resolve whether specific variants are pathogenic or not (17). The more information there is about a particular protein, the more accurate the prediction is likely to be. We have compared our functional data with predictions using the SIFT algorithm (15, 16) and with the method of Grantham (18) (Supporting Data; Part 3, Figures 6 and 7). Some predicted tolerated changes were found to affect TSC1-TSC2 function; while no effect on function could be established for some changes that were predicted not to be tolerated (Supporting Data; Part 1, Tables 1 and 2). This indicates that predictive methods are not reliable for molecular genetic diagnostics and that functional tests provide important, extra insight into the effects of different amino acid changes.

Numerous studies using truncated TSC2 proteins, including our own (19), have indicated that the N-terminal region of TSC2 is important for the interaction with TSC1. Interaction between TSC1 and TSC2 stabilises TSC1 in a soluble, TSC2-bound form, increasing the amount of TSC1 detected by immunoblotting (20). We have quantified the effects of the different TSC2 variants on TSC1 expression levels. The results of this analysis are shown in the Supporting Data; Part 3, Figure 8. TSC1 expression levels were reduced in the presence of pathogenic TSC2 variants with amino acid changes to the N-terminal region of the protein (approximate amino acids 100 - 1000). In contrast, changes to the C-terminal region of TSC2 (amino acids 1000 - 1807) did not have such a large effect on TSC1 expression levels. Nevertheless, amino acid substitutions within this region still resulted in inactivation of the TSC1-TSC2 complex, as assayed by

estimating the T389 phosphorylation of S6K. So far, we have characterised 27 amino acid changes between amino acids 1000 and 1807 that inactivate the TSC1-TSC2 complex, indicating that the region of TSC2 necessary for GAP activity is likely to extend further than the domain defined by homology with rap1GAP (2).

The exact role of TSC1 within the TSC1-TSC2 complex is not completely clear (4, 21) and at the start of the project, it was not known whether missense mutations in the *TSC1* gene could cause TSC. We analysed a series of putative pathogenic TSC1 missense variants, and showed that *TSC1* missense mutations do cause TSC (22). We extended our study to include more unclassified TSC1 variants listed in the LOVD *TSC1* mutation database (Supporting Data; Part 2 and Part 3, Figure 1). Our analysis indicates that pathogenic TSC1 amino acid changes are clustered to a conserved ~300 amino acid region close to the N-terminal of the protein. These substitutions affect the turn-over and stability of TSC1 (Supporting Data; Part 2).

*4. Development of a rapid test for TSC1-TSC2 function*.

One of the principle aims of the project was to improve the methodology of the functional assays. At the start of the project our approach was to perform several different tests to analyse TSC1-TSC2 binding and the effect of TSC1-TSC2 on TORC1. In addition, we set up an in-cell Western (ICW) assay for analysing TSC2 variants (23). ICW assays have the advantage of being reproducible, amenable to automation and simple to perform. However, ICW requires large quantities of antibody, making the test relatively expensive. Therefore, we decided to focus on improving our immunoblot assay. We now use a new SDS-PAGE gel-buffer system that has overcome previous reliability problems and reduced the time required for running and blotting. The new immunoblotting protocol is quicker and easier than the other methods and provides information on the stability of the individual variants being tested as well as on their biochemical activity. We have been able to increase the numbers of variants that can be analysed, and to reduce the cost per analysed variant. Our current assay allows us to analyse the TSC1-TSC2 interaction and TORC1 activity for 25 variants on a single gel. Nevertheless, functional testing of TSC1 and TSC2 variants remains expensive and time-consuming. In particular, deriving the mutants by site-directed mutagenesis is a significant bottleneck. However, we have been able to reduce the quantity of DNA required for sequencing the variant constructs and performing the transfections from ~100 µg to ~20 µg, resulting in more savings in time and materials.

The improvements in reliability between experiments and the ability to quantify the intensity of the signals obtained by immunoblotting (24) has made it possible to estimate the differences between the variants being tested, wild-type TSC2 and known inactive, pathogenic variants. Our current approach is to compare new variants to wild-type TSC2 and the TSC2 R611Q mutant in at least 3 independent experiments. If the ratio of the signals of T389-phosphorylated S6K to total S6K (T389/S6K ratio) for a specific variant is significantly higher than wild-type TSC2 (t-test, $p < 0.05$) and not significantly different from the R611Q mutant (t-test, $p > 0.05$) then we classify the variant as mutant (pathogenic). If the T389/S6K ratio for a specific variant is significantly lower than the R611Q mutant (t-test, $p < 0.05$) and not significantly different from wild-type TSC2 (t-test, $p > 0.05$) then we classify the amino acid change as functionally neutral. In each case the T389/S6K ratios for wild-type TSC2 and the R611Q mutant must be significantly different (t-test, $p < 0.05$). If the T389/S6K is significantly different from both wild-type TSC2 and the R611Q mutant, we classify the variant as "mild" (Supporting Data; Part 1, Table 2). This means that it is possible that the variant has an intermediate level of activity.

**Key Research Accomplishments (23/1/09 - 31/7/09)**

1. Derived and analysed 31 unclassified TSC2 variants: 16 pathogenic; 7 neutral; 8 still unclassified/analysis not complete (Supporting Data; Part 1, Table 2).
2. Derived and analysed 12 unclassified TSC1 variants: 3 pathogenic; 7 neutral; 2 still unclassified/analysis not complete (Supporting Data; Part 1, Table 1).
3. Improvements in assay cost, throughput and reproducibility.
4. Identification of variants with an intermediate effect on TSC1-TSC2 activity.

**Reportable Outcomes (since the start of the project)**

*1. Manuscripts*:
Nellist M, Sancak O, Goedbloed M, Adriaans, Wessels M, Maat-Kievit A, Baars M, Dommering C, van den Ouweland A and Halley D. "Functional characterisation of the TSC1-TSC2 complex te assess multiple *TSC2* variants identified in single families

affected by tuberous sclerosis complex". BMC Med. Genet. (2008) 9:10 doi:10.1186/1471-2350-9-10.

Nellist M, van den Heuvel D, Schluep D, Exalto C, Goedbloed M, Maat-Kievit A, van Essen T, van Spaendonck-Zwarts, Jansen F, Helderman P, Bartalini G, Vierimaa O, Penttinen M, van den Ende J, van den Ouweland A and Halley D. "Missense mutations to the *TSC1* gene cause tuberous sclerosis complex". Eur. J. Hum. Genet. (2009) 17: 319 - 328.

Coevoets R, Arican S, Hoogeveen-Westerveld M, Simons E, van den Ouweland A, Halley D and Nellist M. "A reliable cell-based assay for testing unclassified *TSC2* gene variants." Eur. J. Hum. Genet. (2009) 17: 301 - 310.

Mozaffari M, Hoogeveen-Westerveld M, Kwiatkowski D, Sampson J, Ekong R, Povey S, den Dunnen J, van den Ouweland A, Halley D and Nellist M. "Identification of a region required for TSC1 stability by functional analysis of *TSC1* missense mutations found in individuals with tuberous sclerosis complex". BMC Med. Genet. (submitted)

*2. Abstracts/Presentations*:

Nellist M "Functional analysis of TSC1 and TSC2 variants" 9th International Research Conference on Tuberous Sclerosis Complex, 11 - 13th September 2008, University of Sussex, Brighton, U.K. (invited talk).

Mozaffari M, Hoogeveen-Westerveld M and Nellist M "Functional analysis of *TSC1* missense mutations identified in individuals with tuberous sclerosis complex" Poster Session, 6th November 2008, LAM/TSC Seminar series, Harvard Medical School, Boston, Massachusetts, U.S.A. (poster presentation).

Nellist M "Genetic basis of tuberous sclerosis complex" 8th Dutch Endo-Neuro-Psycho Meeting, 3rd - 5th June 2009, Doorwerth, The Netherlands. (invited talk)

Nellist M "Functional analysis of TSC1 and TSC2 variants identified in individuals with tuberous sclerosis complex" 9th July 2009, Department of Neuropathology, University Hospital, Bonn, Germany (invited talk)

*3. Degrees awarded* (supported by this award):

none

*4. Databases*:

Data generated by this study has been added to the LOVD *TSC1* and *TSC2* mutation databases (7, 8).

## Conclusions

Pathogenic, non-truncating *TSC1* and *TSC2* mutations can be distinguished from non-pathogenic changes by studying the effects of the changes on the TSC1-TSC2 protein complex, or on splicing of the *TSC1* and *TSC2* mRNAs. Functional characterisation of unclassified *TSC1* and *TSC2* variants complements existing diagnostic tests and enables appropriate clinical care and counselling for more TSC patients and their relatives.

Characterisation of multiple TSC1 and TSC2 variants has helped to define structural and catalytic domains in TSC1 and TSC2 and should help provide insight into the folding and three-dimensional structure of the TSC1-TSC2 complex, as well as the regulation and mechanism of GAP catalysis. The stability of different variants, the strength of the TSC1-TSC2 interaction and the GAP activity all influence the biological activity of the TSC1-TSC2 complex.

According to the *in vitro* assays, some truncating TSC1 and non-truncating TSC1 and TSC2 mutations retain some ability to inhibit TORC1 activity and could therefore be associated with a less severe TSC phenotype.

In total, we have tested, or are in the process of testing, 98 TSC2 variants and 38 TSC1 variants. So far, we have classified 60 TSC2 variants and 12 TSC1 variants as mutant or pathogenic, and 29 TSC2 variants and 19 TSC1 variants as neutral.

*Innovations*:

The functional characterisation of TSC1 and TSC2 variants has extended the current diagnostic service that can be offered to TSC patients and their families. Further,

it has helped identify and characterise the structural and functional domains in TSC1 and TSC2, and provided insight into specific genotype-phenotype correlations in TSC.

*Impact*:

Tests to distinguish pathogenic and non-pathogenic *TSC1* and *TSC2* variants are of direct importance to the individuals who carry or may inherit these variants. The data generated by this study will be of benefit to individuals and families affected by TSC in whom 'unclassified variants' have been identified.

The study has already enabled families to obtain more certainty about their condition and to be be able to seek appropriate and accurate care and counselling. In addition, comparison of the biochemical effects of different pathogenic variants with the corresponding phenotypes in the affected individuals has provided additional insight into possible genotype-phenotype correlations in TSC. A very interesting possibility is that specific non-truncating mutations could be associated with a less severe TSC phenotype.

Finally, the identification of amino acids essential for TSC1-TSC2 function has provided more insight into the molecular mechanisms of TSC1-TSC2 function. These data will be useful not only for assessing and testing the accuracy of current predictive methods of amino acid analysis but also in the development of new, improved predictive methods.

**References**

1. Gomez M, Sampson J, Whittemore V, eds. *The tuberous sclerosis complex*. Oxford University Press, Oxford, UK, 1999.

2. The European Chromosome 16 TSC Consortium. Identification and characterisation of the tuberous sclerosis gene on chromosome 16. Cell 75 (1993) 1305-1315.

3. van Slegtenhorst M, de Hoogt R, Hermans C, Nellist M, Janssen LAJ, Verhoef S, Lindhout D, van den Ouweland AMW, Halley DJJ, Young J, Burley M, Jeremiah S,

Woodward K, Nahmias J, Fox M, Ekong R, Wolfe J, Povey S, Osborne J, Snell RG, Cheadle JP, Jones AC, Tachataki M, Ravine D, Sampson JR, Reeve MP, Richardson P, Wilmer F, Munro C, Hawkins TL, Sepp T, Ali, JBM, Ward S, Green AJ, Yates JRW, Short MP, Haines JH, Jozwiak S, Kwiatkowska J, Henske EP and Kwiatkowski DJ. Identification of the tuberous sclerosis gene (*TSC1*) on chromosome 9q34. Science (1997) 277 805-808.

4. Huang J and Manning BD: The TSC1-TSC2 complex: a molecular switchboard controlling cell growth. Biochem J. (2008) 412 179-190.

5. Sancak O, Nellist M, Goedbloed M, Elfferich P, Wouters C, Maat-Kievit A, Zonnenberg B, Verhoef S, Halley D and van den Ouweland A. Mutational analysis of the TSC1 and TSC2 genes in a diagnostic setting: Genotype - phenotype correlations and comparison of diagnostic DNA techniques in Tuberous Sclerosis Complex. Eur. J. Hum. Genet. (2005) 13 731-741.

6. Nellist M, Sancak O, Goedbloed MA, Rohe C, van Netten D, Mayer K, Tucker-Williams A, van den Ouweland AMW and Halley DJJ. Distinct effects of single amino acid changes to tuberin on the function of the tuberin-hamartin complex. Eur. J. Hum. Genet. (2005) 13 59-68.

7. Tuberous sclerosis database - Leiden Open Variation Database [www.chromium.liacs.nl/lovd/index.php?select_db=TSC1].

8. Tuberous sclerosis database - Leiden Open Variation Database [www.chromium.liacs.nl/lovd/index.php?select_db=TSC2].

9. Ramantani G, Niggemann P, Hahn G, Nake A, Fahsold R and Lee-Kirsch MA Unusual radiological presentation of tuberous sclerosis complex with leptomeningeal angiomatosis associated with a hypomorphic mutation in the *TSC2* gene. J. Child Neurol. (2009) 24 333-337.

10. NetGene2 Server [www.cbs.dtu.dk/services/NetGene2].

11. BDGP: Splice Site Prediction by Neural Network [www.fruitfly.org/seq_tools/splice.html].

12. Human Splicing Finder [www.umd.be/HSF/HSF.html].

13. Jansen A, Sancak O, D'Agostino D, Badhwar A, Roberts P, Gobbi G, Wilkinson R, Melanson D, Tampieri D, Koenekoop R, Gans M, Maat-Kievit A, Goedbloed M, van den Ouweland AMW, Nellist M, Pandolfo M, McQueen M, Sims K, Thiele E, Dubeau F, Andermann F, Kwiatkowski DJ, Halley DJJ and Andermann E. Mild form of tuberous sclerosis complex is associated with TSC2 R905Q mutation. Ann. Neurol. (2006) 60 528-539.

14. Pollizzi K, Malinowska-Kolodzei I, Doughty C, Betz C, Ma J, Goto J and Kwiatkowski DJ. A hypomorphic allele of *Tsc2* highlightd the role of TSC1/TSC2 in signaling to AKT and models mild human *TSC2* alleles. Hum. Molec. Genet. (2009) 18 2378-2387.

15. Ng PC and Henikoff S. Predicting the effects of amino acid substitutions on protein function. Annu. Rev. Genomics Hum. Genet. (2006) 7 61-80.

16. Ng PC and Henikoff S. Accounting for human polymorphisms predicted to affect protein function. Genome Res. (2002) 12 436-446.

17. Mathe E, Olivier M, Kato S, Ishioka C, Hainaut P and Tavtigian SV. Computational approaches for predicting the biological effect of p53 missense mutations: a comparison of three sequence analysis based methods. Nuc. Acids. Res. (2006) 34 1317-1325.

18. Grantham R. Amino acid difference formula to help explain protein evolution. Science (1974) 185 862-864.

19. Nellist M, Verhaaf B, Goedbloed M, Reuser A, van den Ouweland A and Halley D. *TSC2* missense mutations inhibit tuberin phosphorylation and prevent formation of the tuberin-hamartin complex. Hum. Molec. Genet. (2001) 10 2889-2898.

20. Nellist M, van Slegtenhorst M, Goedbloed M, van den Ouweland A, Halley D and van der Sluijs P. J. Biol. Chem. (1999) 274 35647-35652.

21. Rosner M, Hanneder M, Siegel N, Valli A, Fuchs C and Hengstschlager M. The tuberous sclerosis gene products hamartin and tuberin are multifunctional proteins with a wide spectrum of interacting partners. Mut. Res. (2008) 658 234-246.

22. Nellist M, van den Heuvel D, Schluep D, Exalto C, Goedbloed M, Maat-Kievit A, van Essen T, van Spaendonck-Zwarts, Jansen F, Helderman P, Bartalini G, Vierimaa O, Penttinen M, van den Ende J, van den Ouweland A and Halley D. Missense mutations to the *TSC1* gene cause tuberous sclerosis complex. Eur. J. Hum. Genet. (2009) 17 319-328.

23. Coevoets R, Arican S, Hoogeveen-Westerveld M, Simons E, van den Ouweland A, Halley D and Nellist M. A reliable cell-based assay for testing unclassified *TSC2* gene variants. Eur. J. Hum. Genet. (2009) 17 301-310.

24. Schutz-Geschwender A, Zhang Y, Holt T, McDermitt D and Olive DM (2004) Quantitative, two-color Western blot detection with infrared fluorescence. http://www.licor.com/bio/PDF/IRquant.pdf (25 Jul.2006).

**Supporting Data**

## Part 1: Summary Tables

**Table 1. Functional classification of TSC1 variants.** All variants were tested at least 3 times. Variants analysed in the period 23/1/09 - 31/7/09 are indicated in bold. SIFT refers to the "sorting intolerant from tolerant" protein prediction program (15, 16). Putative splice site mutations are indicated as "splicing mutation?"

| nucleotide change | effect on splicing | amino acid change | effect on TSC1-TSC2? | status of amino acid change | SIFT |
|---|---|---|---|---|---|
| c.149T>C | none predicted | p.L50P | yes | mutant | not tolerated |
| c.153A>C | none predicted | p.E51D | no | neutral | tolerated |
| c.182T>C | none predicted | p.L61P | yes | mutant | not tolerated |
| **c.215T>C** | **none predicted** | **p.L72P** | **yes** | **mutant** | **not tolerated** |
| **c.227T>A** | **none predicted** | **p.I76N** | **yes** | **mutant** | **not tolerated** |
| **c.250G>A** | **none predicted** | **p.A84T** | **no** | **neutral** | **tolerated** |
| c.278T>G | none predicted | p.L93R | yes | mutant | not tolerated |
| c.350T>C | none predicted | p.L117P | yes | mutant | not tolerated |
| **c.362A>G** | **predicted** | **p.K121R** | **no** | **neutral (splice mutation?)** | **tolerated** |
| c.379_381delTGT | predicted | p.128delV | yes | mutant | no prediction |
| c.397G>T | none predicted | p.V133F | yes | mutant | not tolerated |

| nucleotide change | effect on splicing | amino acid change | effect on TSC1-TSC2? | status of amino acid change | SIFT |
|---|---|---|---|---|---|
| c.539T>C | none predicted | p.L180P | yes | mutant | not tolerated |
| c.568C>T | none predicted | p.R190C | no | neutral | not tolerated |
| c.569G>C | none predicted | p.R190P | yes | mutant | not tolerated |
| c.572T>A | none predicted | p.L191H | yes | mutant | not tolerated |
| **c.572T>G** | **none predicted** | **p.L191R** | **yes** | **mutant** | **not tolerated** |
| c.593_595delACT | none predicted | p.NF198delinsI | yes | mutant | no prediction |
| c.671T>G | none predicted | p.M224R | yes | mutant | not tolerated |
| c.737G>A | predicted | p.R246K | no | neutral (splice mutation?) | not tolerated |
| **c.737G>C** | **predicted** | **p.R246T** | **no** | **neutral (splice mutation?)** | **not tolerated** |
| c.913G>A | predicted | p.G305R | no | neutral (splice mutation?) | tolerated |
| c.913G>T | predicted | p.G305W | no | neutral (splice mutation?) | tolerated |
| c.1001C>T | none predicted | p.S334L | no | neutral | tolerated |
| **c.1250C>T** | **none predicted** | **p.T417I** | **no** | **neutral** | **tolerated** |
| c.1433A>G | predicted | p.E478G<br><br>p.479insGN | no<br><br>no | neutral<br><br>neutral | tolerated<br><br>no prediction |

| nucleotide change | effect on splicing | amino acid change | effect on TSC1-TSC2? | status of amino acid change | SIFT |
|---|---|---|---|---|---|
| **c.1460C>G** | **none predicted** | **p.S487C** | **no** | **neutral** | **tolerated** |
| c.1526G>A | none predicted | p.R509Q | no | neutral | tolerated |
| c.1648C>G | none predicted | p.Q550E | no | neutral | tolerated |
| **c.1760A>G** | **none predicted** | **p.K587R** | **no** | **neutral** | **tolerated** |
| c.1974C>G | none predicted | p.D658E | no | neutral | tolerated |
| c.1976C>T | none predicted | p.A659V | no | neutral | tolerated |
| **c.2194C>T** | **none predicted** | **p.H732Y** | **no** | **neutral** | **not tolerated** |
| c.2420T>C | none predicted | p.I807T | no | neutral | tolerated |
| **c.2653C>T** | **none predicted** | **p.R885W** | **no** | **neutral** | **tolerated** |
| **c.2696C>G** | **none predicted** | **p.T899S** | **no** | **neutral** | **tolerated** |
| c.3103G>A | none predicted | p.G1035S | no | neutral | tolerated |
| c.3290G>A | none predicted | p.R1097H | no | neutral | not tolerated |

**Table 2. Functional classification of TSC2 variants.** Variants analysed in the period 23/1/09 - 31/7/09 are indicated in bold. All variants were tested at least 3 times. S6K-T389 phosphorylation (ratio to total protein, as estimated by immunoblotting) was determined per variant and compared to the values for the wild-type TSC2 and the R611Q pathogenic variant from the same set of experiments using Student's t-test. A p value $< 0.05$ was considered a significant difference. For each set of experiments the wild-type TSC2 and R611Q mutant were significantly different ($p < 0.05$). Variants significantly different from wild-type, but not significantly different from the R611Q mutant were classified as mutant. Variants significantly different from the R611Q mutant, but not significantly different from wild-type were classified as neutral. Variants that were significantly different from both the wild-type and the R611Q mutant were classified as "mild". In each case these variants appeared to be more active than the R611Q mutant, but less active than wild-type TSC2. Putative splice site mutations are indicated in the table as "splice mutation?". Amino acid numbering in parentheses corresponds to the TSC2 isoform lacking the amino acids encoded by the alternatively spliced exon 31.

| nucleotide change | effect on splicing? | amino acid change | effect on TSC1-TSC2 complex? | | | SIFT |
|---|---|---|---|---|---|---|
| | | | t-test vs. wild-type | t-test vs. R611Q | status | |
| **c.170G>A** | **none predicted** | **p.R57H** | **0.0239** | **0.0086** | **mutant (mild)** | **not tolerated** |
| c.185G>A | none predicted | p.G62E | 0.2745 | 0.0039 | neutral | tolerated |
| c.292C>T | none predicted | p.R98W | 0.0092 | 0.2474 | mutant | not tolerated |
| c.395C>G | none predicted | p.S132C | 0.3209 | 0.0354 | neutral | tolerated |
| c.429C>G | none predicted | p.F143L | 0.1401 | 0.0079 | neutral | tolerated |
| c.586G>A | none predicted | p.A196T | 0.4751 | 0.0405 | neutral | tolerated |
| **c.646G>A** | **none predicted** | **p.E216K** | **0.1883** | **0.0183** | **neutral** | **tolerated** |
| c.656T>C | none predicted | p.L219P | 0.0226 | 0.1126 | mutant | not tolerated |
| c.730T>C | none predicted | p.C244R | 0.0112 | 0.0763 | mutant | not tolerated |
| **c.782G>C** | **none predicted** | **p.R261P** | **not done yet** | **not done yet** | **testing not complete** | **tolerated** |
| **c.781C>T** | **none predicted** | **p.R261W** | **not done yet** | **not done yet** | **testing not complete** | **not tolerated** |
| **c.825C>A** | **none predicted** | **p.N275K** | **0.2749** | **0.0174** | **neutral** | **tolerated** |
| c.824delACA | none predicted | p.275delN | 0.0056 | 0.8181 | mutant | no prediction |
| **c.1001T>C** | **none predicted** | **p.V334A** | **0.0167** | **0.0103** | **mutant (mild)** | **not tolerated** |
| **c.1001T>G** | **none predicted** | **p.V334G** | **0.0100** | **0.1651** | **mutant** | **not tolerated** |
| c.1019T>C | none predicted | p.L340P | 0.0062 | 0.0147 | mutant (mild) | not tolerated |
| c.1100G>A | none predicted | p.R367Q | 0.4878 | 0.0107 | neutral | tolerated |

| nucleotide change | effect on splicing? | amino acid change | effect on TSC1-TSC2 complex? | | | SIFT |
|---|---|---|---|---|---|---|
| | | | t-test vs. wild-type | t-test vs. R611Q | status | |
| c.1118A>C | predicted | p.Q373P | 0.8106 | 0.0025 | neutral (splice mutation?) | tolerated |
| c.1235A>T | yes | p.E412V<br><br><br>p.412del8 | 0.1001<br><br><br>0.0277 | 0.0183<br><br><br>0.4891 | neutral<br><br><br>mutant (splice) | not tolerated<br><br><br>no prediction |
| **c.1255C>T** | **predicted** | **p.P419S** | **0.6898** | **0.0001** | **neutral (splice mutation?)** | **not tolerated** |
| c.1366G>A | none predicted | p.E456K | 0.1928 | 0.0292 | neutral | tolerated |
| **c.1378G>A** | **none predicted** | **p.A460T** | **not done yet** | **not done yet** | **testing not complete** | **tolerated** |
| **c.1385G>A** | **none predicted** | **p.R462H** | **0.0083** | **0.1793** | **mutant (mild)** | **not tolerated** |
| **c.1385_1386delinsCT** | **none predicted** | **p.R462P** | **0.0130** | **0.0145** | **mutant (mild)** | **not tolerated** |
| c.1397T>C | none predicted | p.L466P | 0.0214 | 0.0979 | mutant | tolerated |
| c.1574A>G | none predicted | p.N525S | 0.3367 | 0.0102 | neutral | tolerated |
| c.1736del78 | none predicted | p.580del26 | 0.0113 | 0.7135 | mutant | no prediction |
| c.1791insCAC | none predicted | p.597insH | 0.0339 | 0.0981 | mutant | no prediction |
| c.1792T>C | none predicted | p.Y598H | 0.0184 | 0.2322 | mutant | tolerated |
| c.1796A>T | none predicted | p.K599M | 0.3791 | 0.0162 | neutral | tolerated |
| c.1820C>A | none predicted | p.A607E | 0.0141 | 0.9254 | mutant | tolerated |
| c.1819G>T | none predicted | p.A607S | 0.2520 | 0.0254 | neutral | tolerated |

| nucleotide change | effect on splicing? | amino acid change | effect on TSC1-TSC2 complex? | | | SIFT |
|---|---|---|---|---|---|---|
| | | | t-test vs. wild-type | t-test vs. R611Q | status | |
| c.1819G>A | none predicted | p.A607T | 0.5394 | 0.0041 | neutral | tolerated |
| c.1826_1828dup | none predicted | p.609insS | 0.0017 | 0.0898 | mutant | no prediction |
| c.1832G>A | none predicted | p.R611Q | < 0.05 (in all cases) | - | mutant | not tolerated |
| c.1831C>T | none predicted | p.R611W | 0.0184 | 0.1991 | mutant | not tolerated |
| c.1841C>A | none predicted | p.A614D | 0.0058 | 0.9886 | mutant | tolerated |
| c.1844T>C | none predicted | p.F615S | 0.0027 | 0.1156 | mutant | tolerated |
| **c.1865G>C** | **none predicted** | **p.R622C** | **0.6130** | **0.0398** | **neutral** | **not tolerated** |
| c.1864C>T | none predicted | p.R622W | 0.0179 | 0.0610 | mutant | not tolerated |
| **c.2078T>C** | **none predicted** | **p.L693P** | **0.0178** | **0.4665** | **mutant** | **not tolerated** |
| c.2087G>A | none predicted | p.C696Y | 0.0160 | 0.3228 | mutant | not tolerated |
| c.2306T>A | none predicted | p.V769E | 0.0092 | 0.2052 | mutant | tolerated |
| **c.2363T>G** | **none predicted** | **p.M788R** | **0.0042** | **0.1471** | **mutant** | **not tolerated** |
| c.2458_2460del | none predicted | p.820delI | 0.0046 | 0.4310 | mutant | no prediction |
| c.2476C>A | none predicted | p.L826M | 0.0757 | 0.0466 | neutral | not tolerated |
| **c.2666C>T** | **none predicted** | **p.A889V** | **0.0045** | **0.0171** | **mutant (mild)** | **not tolerated** |
| c.2690T>C | none predicted | p.F897S | 0.0188 | 0.5847 | mutant | not tolerated |
| c.2713C>G | none predicted | p.R905G | 0.0396 | 0.0769 | mutant | not tolerated |

| nucleotide change | effect on splicing? | amino acid change | effect on TSC1-TSC2 complex? | | | SIFT |
|---|---|---|---|---|---|---|
| | | | t-test vs. wild-type | t-test vs. R611Q | status | |
| c.2714G>A | none predicted | p.R905Q | 0.0005 | 0.0109 | mutant (mild) | not tolerated |
| c.2713C>T | none predicted | p.R905W | 0.0009 | 0.0722 | mutant | not tolerated |
| c.2747T>G | none predicted | p.L916R | 0.0002 | 0.0613 | mutant | not tolerated |
| **c.2853A>T** | **none predicted** | **p.R951S** | **0.1692** | **0.0136** | **neutral** | **tolerated** |
| c.2963G>C | none predicted | p.R988P | 0.7014 | 0.0437 | neutral | tolerated |
| c.2978C>T | none predicted | p.T993M | 0.1499 | 0.0185 | neutral | tolerated |
| **c.3082G>A** | **none predicted** | **p.D1028N** | **0.0028** | **0.1982** | **mutant** | **not tolerated** |
| c.3095G>C | none predicted | p.R1032P | 0.0474 | 0.0565 | mutant | not tolerated |
| **c.3106T>C** | **none predicted** | **p.S1036P** | **0.0008** | **0.1008** | **mutant** | **not tolerated** |
| c.3182T>C | none predicted | p.L1061P | 0.0025 | 0.7156 | mutant | not tolerated |
| c.3203C>A | none predicted | p.T1068I | 0.0271 | 0.1148 | mutant | not tolerated |
| c.3224C>T | none predicted | p.T1075I | 0.1422 | 0.0169 | neutral | not tolerated |
| **c.3364C>T** | **none predicted** | **p.R1122C** | **not done yet** | **not done yet** | **testing not complete** | **tolerated** |
| **c.3476G>T** | **none predicted** | **p.R1159L** | **0.5083** | **0.0087** | **neutral** | **tolerated** |
| **c.3476G>A** | **none predicted** | **p.R1159Q** | **0.5897** | **0.0269** | **neutral** | **tolerated** |
| **c.3475C>T** | **none predicted** | **p.R1159W** | **0.3158** | **0.0354** | **neutral** | **tolerated** |
| c.3596T>G | none predicted | p.V1199G | 0.0086 | 0.9323 | mutant | tolerated |
| **c.3598C>T** | **none predicted** | **p.R1200W** | **0.0026** | **0.5056** | **mutant** | **not tolerated** |

| nucleotide change | effect on splicing? | amino acid change | effect on TSC1-TSC2 complex? | | | SIFT |
|---|---|---|---|---|---|---|
| | | | t-test vs. wild-type | t-test vs. R611Q | status | |
| c.3605C>A | none predicted | p.P1202H | 0.0082 | 0.1733 | mutant | tolerated |
| c.3943C>G | none predicted | p.P1313A (P1292A) | 0.3097 | 0.0020 | neutral | tolerated |
| **c.4105C>T** | **none predicted** | **p.R1369W (R1346W)** | **not done yet** | **not done yet** | **testing not complete** | **tolerated** |
| c.4225C>T | none predicted | p.R1409W (R1386W) | 0.8566 | 0.0009 | neutral | tolerated |
| c.4298C>T | none predicted | p.S1433L (S1410L) | 0.3846 | 0.0098 | neutral | tolerated |
| c.4316G>A | none predicted | p.G1439D (G1416D) | 0.4211 | 0.0051 | neutral | tolerated |
| **c.4490C>G** | **none predicted** | **p.P1497R (P1474R)** | **0.0007** | **0.1850** | **mutant** | **not tolerated** |
| c.4489C>T | none predicted | p.P1497S (P1474S) | 0.0171 | 0.0272 | mutant (mild) | tolerated |
| **c.4489C>A** | **none predicted** | **p.P1497T (P1474T)** | **0.0283** | **0.8124** | **mutant** | **not tolerated** |
| c.4525_4527del | none predicted | p.1510delF (1487delF) | 0.6286 | 0.0037 | neutral | no prediction |
| c.4601T>A | none predicted | p.L1534H (L1511H) | 0.0194 | 0.1942 | mutant | not tolerated |
| c.4604A>C | none predicted | p.D1535A (D1512A) | 0.0001 | 0.8758 | mutant | not tolerated |
| c.4643T>C | none predicted | p.L1548P (L1525P) | 0.0241 | 0.7355 | mutant | not tolerated |
| c.4700G>T | none predicted | p.G1567V (G1544V) | 0.0019 | 0.7236 | mutant | not tolerated |
| c.4726del57 | none predicted | p.1575del19 (1552del19) | 0.0030 | 0.7628 | mutant | not tolerated |
| c.4735G>A | none predicted | p.G1579S (G1556S) | 0.0011 | 0.0835 | mutant | not tolerated |
| c.4918C>T | none predicted | p.H1640Y (H1617Y) | 0.0011 | 0.6501 | mutant | not tolerated |

| nucleotide change | effect on splicing? | amino acid change | effect on TSC1-TSC2 complex? | | | SIFT |
|---|---|---|---|---|---|---|
| | | | t-test vs. wild-type | t-test vs. R611Q | status | |
| **c.4927A>C** | **none predicted** | **p.N1643H (N1620H)** | **not done yet** | **not done yet** | **testing not complete** | **not tolerated** |
| **c.4928A>T** | **none predicted** | **p.N1643I (N1620I)** | **0.0077** | **0.0732** | **mutant** | **not tolerated** |
| **c.4929C>G** | **none predicted** | **p.N1643K (N1620K)** | **0.0041** | **0.1613** | **mutant** | **not tolerated** |
| c.4928A>G | none predicted | p.N1643S (N1620S) | 0.0175 | 0.9750 | mutant | not tolerated |
| c.4937T>G | none predicted | p.V1646G (V1623G) | 0.0476 | 0.8984 | mutant | not tolerated |
| c.5057A>C | none predicted | p.Q1686P (Q1663P) | 0.0234 | 0.0519 | mutant | tolerated |
| c.5138G>A | none predicted | p.R1713H (R1690H) | 0.0020 | 0.4437 | mutant | not tolerated |
| c.5228G>A | none predicted | p.R1743Q (R1720Q) | 0.0004 | 0.6100 | mutant | not tolerated |
| c.5227C>T | none predicted | p.R1743W (R1720W) | 0.0032 | 0.8623 | mutant | not tolerated |
| **c.5186del18** | **none predicted** | **p.1746del6 (1723del6)** | **0.0001** | **0.4383** | **mutant** | **no prediction** |
| **c.5376G>C** | **none predicted** | **p.Q1792H (Q1769H)** | **not done yet** | **not done yet** | **testing not complete** | **not tolerated** |
| c.5383C>T | none predicted | p.R1795C (R1772C) | 0.0967 | 0.0324 | neutral | not tolerated |
| c.5386C>T | none predicted | p.L1796I (L1773I) | 0.7698 | 0.0008 | neutral | tolerated |

**Supporting Data Part 2: Publications and submitted manuscripts**

## Publications

Nellist M, Sancak O, Goedbloed M, Adriaans, Wessels M, Maat-Kievit A, Baars M, Dommering C, van den Ouweland A and Halley D. "Functional characterisation of the TSC1-TSC2 complex te assess multiple *TSC2* variants identified in single families affected by tuberous sclerosis complex". BMC Med. Genet. (2008) 9:10 doi:10.1186/1471-2350-9-10.

Nellist M, van den Heuvel D, Schluep D, Exalto C, Goedbloed M, Maat-Kievit A, van Essen T, van Spaendonck-Zwarts, Jansen F, Helderman P, Bartalini G, Vierimaa O, Penttinen M, van den Ende J, van den Ouweland A and Halley D. "Missense mutations to the *TSC1* gene cause tuberous sclerosis complex". Eur. J. Hum. Genet. (2008) doi:10.1038/ejhg.2008.170.

Coevoets R, Arican S, Hoogeveen-Westerveld M, Simons E, van den Ouweland A, Halley D and Nellist M. "A reliable cell-based assay for testing unclassified *TSC2* gene variants." Eur. J. Hum. Genet. (2008) doi:10.1038/ejhg.2008.184.

Mozaffari M, Hoogeveen-Westerveld M, Kwiatkowski D, Sampson J, Ekong R, Povey S, van den Ouweland A, Halley D and Nellist M. "Identification of a region required for TSC1 stability by functional analysis of *TSC1* missense mutations identified in individuals with tuberous sclerosis complex." [submitted BMC Med. Genet; see below].

**Title page:**

# Identification of a region required for TSC1 stability by functional analysis of *TSC1* missense mutations found in individuals with tuberous sclerosis complex

Melika Mozaffari[1], Marianne Hoogeveen-Westerveld[1], David Kwiatkowski[2], Julian Sampson[3], Rosemary Ekong[4], Sue Povey[4], Johan den Dunnen[5], Ans van den Ouweland[1], Dicky Halley[1] and Mark Nellist[1,6]

[1] Department of Clinical Genetics, Erasmus Medical Centre, 3015 GE Rotterdam, The Netherlands

[2] Division of Experimental Medicine and Medical Oncology, Brigham and Womens Hospital, Boston MA 02115, United States of America

[3] Institute of Medical Genetics, University of Wales College of Medicine, Heath Park, Cardiff CF4 4XN, United Kingdom

[4] Research Department of Genetics, Evolution and Environment, University College London Wolfson House, 4 Stephenson Way, London, NW1 2HE, United Kingdom

[5] Department of Human and Clinical Genetics, Leiden University Medical Centre, 2333ZC Leiden, The Netherlands

[6] To whom correspondence should be addressed: Dr. Mark Nellist, Department of Clinical Genetics, Erasmus Medical Centre, Dr. Molewaterplein 50, 3015 GE Rotterdam, The Netherlands, Tel: +31 10 7043357; Fax: +31 10 7044736; email: m.nellist@erasmusmc.nl

**Running title**: Functional analysis of TSC1 variants


## Abstract

### *Background*

Tuberous sclerosis complex (TSC) is an autosomal dominant disorder characterised by the development of hamartomas in a variety of organs and tissues. The disease is caused by mutations in either the *TSC1* gene on chromosome 9q34, or the *TSC2* gene on chromosome 16p13.3. The *TSC1* and *TSC2* gene products, TSC1 and TSC2, form a protein complex that inhibits signal transduction to the downstream effectors of the mammalian target of rapamycin (mTOR). Recently it has been shown that missense mutations to the *TSC1* gene can cause TSC.

### *Methods*

We have used *in vitro* biochemical assays to investigate the effects on TSC1 function of *TSC1* missense variants submitted to the Leiden Open Variation Database.

### *Results*

We identified specific amino acid substitutions in the N-terminal region of TSC1 that result in reduced steady state levels of the protein and lead to increased mTOR signalling.

### *Conclusion*

Our results suggest that the N-terminal region of TSC1 is important for TSC1 function and for maintaining the activity of the TSC1-TSC2 complex.



**Keywords:** tuberous sclerosis complex, TSC1, TSC2

## Background

Tuberous sclerosis complex (TSC) is an autosomal dominant disorder characterised by the development of hamartomas in a variety of organs and tissues, including the brain, skin and kidneys [1,2]. Mutations in either the *TSC1* gene on chromosome 9q34 [3], or the *TSC2* gene on chromosome 16p13.3 [4] cause TSC. In most studies, 75 - 85% of individuals with TSC have been shown to carry a germ-line *TSC1* or *TSC2* mutation [5-9] and a further 5 - 10% carry *TSC1* or *TSC2* variants where it is not absolutely clear from the genetic data whether the change is disease-causing (a pathogenic variant), or not (a neutral variant). To determine whether these unclassified variants are disease-causing, the effect of the changes on protein function can be investigated [10, 11].

The *TSC1* and *TSC2* gene products, TSC1 and TSC2, interact to form a protein complex [12]. TSC2 contains a GTPase activating protein (GAP) domain and acts on the rheb GTPase to inhibit rheb-GTP-dependent stimulation of the mammalian target of rapamycin (mTOR) [13]. The exact role of TSC1 in the TSC1-TSC2 complex is less clear, but it appears to be required for maintaining the stability, activity and correct intracellular localisation of the complex [14]. Inactivation of the TSC1-TSC2 complex results in activation of mTOR and phosphorylation of the mTOR targets p70 S6 kinase (S6K), ribosomal protein S6 and 4E-BP1 [15]. The effects of amino acid changes to TSC1 or TSC2 on TSC1-TSC2 complex formation, on the activation of rheb GTPase activity by the complex, and on the phosphorylation status of S6K and S6 can be determined [10, 11, 16]. Pathogenic missense changes towards the N-terminus of TSC2 prevent formation of the TSC1-TSC2 complex, while missense changes towards the C-terminus do not prevent TSC1-TSC2 binding but disrupt the rhebGAP activity of TSC2 directly [10]. Pathogenic TSC1 missense changes are rare [5 - 9]. However, recent

studies of TSC1 missense variants identified in bladder cancers [17] and in patients with TSC [11] have shown that TSC1 amino acid substitutions can be pathogenic, reducing steady state levels of TSC1 and leading to increased mTOR activity.

Here, we test 13 *TSC1* variants identified during mutation screening of the *TSC1* in individuals with TSC. Our analysis confirms that pathogenic *TSC1* missense mutations reduce steady state levels of TSC1, and result in increased mTOR signalling. Furthermore, we find that the intracellular localisation of pathogenic and neutral TSC1 variants is distinct. The pathogenic TSC1 amino acid substitutions are clustered within the conserved, hydrophobic N-terminal region of TSC1, indicating that this region plays an important role in TSC1 function.

## Methods

### *Comparative analysis of TSC1 amino acid substitutions*

TSC1 missense variants identified in individuals with TSC, or suspected of having TSC, and submitted to the LOVD *TSC1* mutation database [18, 19] were chosen for analysis. To predict whether the variants were likely to be pathogenic, the amino acid substitutions were evaluated using the BLOSUM 62 and Grantham matrices [20, 21], and a multiple sequence alignment analysis was performed using SIFT software [22, 23]. Hydrophobicity plots and secondary structure predictions were generated using DNAMAN (Lynnon BioSoft), SABLE [24] and PSIPRED [25] software. To determine whether the identified changes were likely to have an effect on splicing, 3 different splice-site prediction programs were used [26 - 28].

### *Generation of constructs and antisera*

Expression constructs encoding myc-tagged TSC1 variants were derived using the QuikChange site-directed mutagenesis kit (Stratagene, La Jolla, CA, U.S.A.). In each case the complete open reading frame of the mutated construct was verified by sequence analysis. Other constructs used in this study have been described previously [10, 11]. Antibodies were described previously [12] or purchased from Cell Signaling Technology (Danvers, MA, U.S.A.), except for a mouse monoclonal antibody against TSC2 which was purchased from Zymed Laboratories (San Francisco, CA, U.S.A.) and a rabbit polyclonal antibody against ubiquitin which was purchased from DAKO (Glostrup, Denmark).

*Effects of TSC1 variants on S6K T389 phosphorylation*

Immunoblot analysis of S6K T389 phosphorylation in cells over-expressing TSC1 variants was performed as described previously [11]. Briefly, 80% confluent HEK 293T cells in 24-well cell culture dishes were transfected with a 4:2:1 mixture of the TSC1, TSC2 and S6K expression constructs (0.7 μg DNA total) in 50 μl Dulbecco's modified Eagle medium (DMEM) containing 2.1 μg polyethyleneimine (Polysciences, Warrington, PA, U.S.A.). Where necessary, an empty expression vector (pcDNA3; Invitrogen, Carlsbad, CA, U.S.A.) was added to make up the total amount of DNA. Twenty-four hours after transfection the cells were washed with cold PBS and lysed in 75 μl 50 mM Tris-HCl pH 8.0, 150 mM NaCl, 50 mM NaF and 1% Triton X100 containing protease inhibitors (Complete, Roche Molecular Biochemicals, Woerden, The Netherlands). After centrifugation (10 000 g, 10 minutes, 4°C), the supernatant and pellet fractions were recovered for immunoblot analysis. The pellet fractions were resuspended in 100 μl 62.5 mM Tris-HCl pH 6.8, 10% glycerol, 300 mM 2-mercaptoethanol, 2% SDS and sonicated (8μm, 15 seconds, 4°C) prior to gel

electrophoresis. Samples were run on 4-12 % SDS-PAGE Criterion gradient gels (BioRad, Hercules, CA, U.S.A.) and blotted onto nitrocellulose. Blots were analysed using near infra-red fluorescent detection on an Odyssey™ Infrared Imager (169 μm resolution, medium quality with 0 mm focus offset) (Li-Cor Biosciences, Lincoln, NE, U.S.A.). The integrated intensities of the protein bands relative to the wild-type TSC1 values were determined in at least 3 separate experiments using the Odyssey™ software (default settings with background correction; 3 pixel width border average method). Signal intensities were compared as described previously [29].

*Proteosome-mediated degradation of TSC1 variants.*

HEK 293T cells were transfected with expression constructs encoding TSC2, S6K and the different TSC1 variants. Twenty-four hours after transfection the culture medium was replaced with DMEM containing either 42 μM MG-132 (Sigma-Aldrich, St. Louis, MO, U.S.A.) or vehicle control. After 4 hours, insulin (200 nM; Sigma-Aldrich) or vehicle control was added to the culture medium and, after a further 30 minute incubation, the cells were harvested and analysed by immunoblotting, as before.

*Immunofluorescent detection of TSC1 variants.*

HEK 293T cells were seeded onto glass coverslips coated with poly-L-lysine (Sigma-Aldrich), transfected with expression constructs encoding the TSC1 variants and processed for immunofluorescent microscopy as described previously [12]. Fixed, permeabilised cells were incubated with a rabbit polyclonal antibody specific for TSC2 [12] and a mouse monoclonal antibody specific for the TSC1 C-terminal myc epitope tag (9B11, Cell Signaling Technology), followed by fluorescein isothiocyanate- and Cy3-coupled secondary antibodies against mouse and rabbit immunoglobulins (DAKO)

respectively. Cells were studied using a Leica DM RXA microscope and Image Pro-Plus version 6 image analysis software.

## Results

*Comparative analysis of TSC1 amino acid substitutions*

We selected 13 TSC1 amino acid substitutions (*TSC1* c.149T>C (p.L50P), c.153A>C (p.E51D), c.182T>C (p.L61P), c.278T>G (p.L93R), c.397G>T (p.V133F), c.568C>T (p.R190C), c.569G>C (p.R190P), c.1001C>T (p.S334L), c.1433A>G (p.E478G), c.1648C>G (p.Q550E), c.1974C>G (p.D658E), c.1976C>T (p.A659V) and c.2420T>C (p.I807T)) that were either possible pathogenic changes, or could not be excluded as neutral variants [18] (Table 1). In this group there was one confirmed *de novo* change, *TSC1* c.182T>C (p.L61P), that was very likely to be pathogenic. In one individual with TSC, 2 *TSC1* missense changes, c.149T>C (p.L50P) and c.2420T>C (p.I807T), were reported. To establish whether either of these changes was responsible for TSC, or whether the combination of both changes was required to inactivate TSC1, we tested a L50P-I807T double variant as well as the L50P and I807T single variants.

To predict whether the amino acid substitutions were likely to be pathogenic, we determined the scores of the BLOSUM 62 [20] and Grantham [21] amino acid substitution matrices for all the missense variants in the LOVD *TSC1* database (Figure 1A and B). These scores give an indication of the differences between amino acid pairs based on amino acid composition, polarity and molecular volume, as well as substitution frequencies. Both matrices indicated that the amino acid substitutions listed in the LOVD *TSC1* database in general become more conservative towards the C-terminal of TSC1. We also performed a SIFT analysis [23] using a multiple sequence alignment of TSC1 derived from 14 different species (human, chimpanzee, maccaca,

cow, dog, horse, mouse, rat, chicken, pufferfish, honey bee, fruitfly, mosquito and fission yeast). The SIFT algorithm combines information from both the chemical structure of the individual amino acids and the evolutionary conservation of the protein to predict for each amino acid residue which substitutions can be tolerated by the protein. The results of the SIFT analysis are shown in Figure 1C and Table 1. Overall, the N-terminal (amino acids 1 - 270) and C-terminal (amino acids 680 - 1164) regions of TSC1 did not tolerate amino acid substitutions while the central region (amino acids 270 - 680) was predicted to be more tolerant (Figure 1C). Of the 13 substitutions selected for this study, 7 were predicted to be tolerated and therefore unlikely to be pathogenic (Table 1). Of these, 5 were located in the central, substitution-tolerant region of TSC1 (amino acids 270 - 680). Six substitutions were predicted not to be tolerated and therefore likely to be pathogenic. All of these changes were located in the substitution-intolerant N-terminal region (amino acids 1 - 270). Finally, we investigated the effect of the substitutions on the hydrophobicity of TSC1 (Figure 1D and E). Three substitutions, p.E51D, p.Q550E and p.D658E, had no significant effect. These were all predicted by the SIFT algorithm to be tolerated changes. Of the remaining tolerated changes, p.S334L, p.E478G and p.A659V increased the hydrophobicity, while the p.I807T substitution had the opposite effect (Figure 1D). In the group of changes not tolerated by the SIFT analysis, the p.L50P, p.L61P, p.L93R and p.V133F substitutions decreased the hydrophobicity while the p.R190C and p.R190P substitutions increased the hydrophobicity (Figure 1E).

Splice site prediction analysis of the *TSC1* nucleotide changes was performed using 3 independent splice site prediction programs. Neither NetGene2 [26] nor Human Splicing Finder [28] predicted any splicing defects for any of the 13 changes. In contrast, NNSPLICE 0.9 [27] predicted that the *TSC1* c.1433A>G (p.E478G) change

would result in the creation of an alternative splice donor site 6 nucleotides downstream of the wild-type exon 14 donor site. Furthermore, the wild-type site was no longer recognised as a splice donor site by the NNSPLICE 0.9 algorithm. If this prediction is correct, the new splice donor site created by the *TSC1* c.1433A>G change would result in the insertion of 2 extra codons (encoding amino acids GN) between codons 479 and 480, in addition to the p.E478G substitution.

*Functional analysis of TSC1 amino acid substitutions*

We characterised the effects of the 13 TSC1 single missense variants and the L50P/I807T double variant on the activity of the TSC1-TSC2 complex. We compared the 14 variants to wild-type TSC1 and the TSC1-L117P pathogenic variant [11]. As shown in Figure 2, the L50P, L61P, L93R, V133F and R190P amino acid substitutions all resulted in reduced levels of TSC1 (Figure 2A and B) and increased mTOR activity, as estimated by the T389 phosphorylation status of S6K (Figure 2A and D). These substitutions all had the same effect on TSC1 as the previously-characterised L117P substitution [11]. In each case, the T389/S6K ratio was significantly different from wild-type TSC1 (unpaired t-test p values all $< 0.05$; Table 1). We did not observe any differences between the L50P variant and the L50P/I807T double variant. Both variants were detected at low levels and did not inhibit S6K phosphorylation as effectively as wild-type TSC1.

The E51D, R190C, S334L, E478G, Q550E, D658E, A659V and I807T variants were detected at comparable levels to wild-type TSC1 (Figure 2A and B) and S6K T389 phosphorylation was reduced to the same levels as in the presence of wild-type TSC1 (Figure 2A and D). In each case, there was no significance difference in the T389/S6K ratio compared to wild-type TSC1 (unpaired t-test p values $> 0.05$; Table 1).

*TSC1 variants are degraded by the proteosome*

We considered two possible reasons for why the TSC1 L50P, L61P, L93R, V133F, R190P and L50P/I807T variants were detected at low levels. One possibility was that the variants were insoluble and therefore not present in the cell lysate fraction analysed by immunoblotting. We analysed the insoluble post cell lysis pellet fractions, but did not detect any of the TSC1 variants in these fractions (data not shown).

The second possibility was that the L50P, L61P, L93R, V133F, R190P and L50P/I807T variants were subject to rapid turn-over and degradation. Therefore, we treated cells expressing wild-type TSC1 or the L50P, L61P, L93R, V133F, R190P, L50P/I807T or L117P variants with the proteosome-inhibitor MG-132 [30]. After 4 hours treatment we observed an increase in the L50P, L61P, L93R, V133F, R190P, L50P/I807T and L117P signals when cells were treated with MG-132 (Figure 3A).

We estimated mTOR activity in MG-132-treated cells by measuring the T389 phosphorylation status of S6K in cells expressing the L50P or L117P variants and treated with MG-132 and/or insulin (Figure 3B - D). The L50P and L117P signals were increased relative to the TSC1 wild-type signals in unstimulated cells treated with MG-132 as well as in cells treated with MG-132 and stimulated with 200 nM insulin for 30 minutes (Figure 3B and C). In (unstimulated and insulin stimulated) cells not treated with MG-132, wild-type TSC1 was detected at higher levels than the L50P and L117P variants, consistent with the analysis shown in Figure 2. In untreated cells, S6K T389 phosphorylation was increased in cells expressing the L50P and L117P variants, compared to cells expressing wild-type TSC1, consistent with the analysis shown in Figure 2. MG-132 treatment did not affect the detected levels of total S6K (Figure 3A), but in cells expressing the L50P and L117P variants, S6K T389 phosphorylation was

increased compared to cells expressing wild-type TSC1, in both insulin-stimulated and unstimulated cells (Figure 3B and D).

*Intracellular localisation of the TSC1 variants*

Exogenous expression of the TSC1 E51D variant resulted in the formation of large, cytoplasmic TSC1 protein aggregates (Figure 4A), consistent with previous results with wild-type TSC1 [31]. Coexpression of TSC2 resulted in a dramatic reduction in the number of aggregates, and both TSC2 and the TSC1 E51D variant were detected throughout the cytoplasm (Figure 4C and D). We observed the same expression pattern for the TSC1 R190C, S334L, E478G, Q550E, D658E, A659V and I807T variants (data not shown).

In contrast to wild-type TSC1 and the E51D, R190C, S334L, E478G, Q550E, D658E, A659V and I807T variants, the L50P variant did not form large cytoplasmic aggregates when over-expressed in HEK 293T cells. Instead, the variant was expressed relatively uniformly throughout the cytoplasm (Figure 4F). This localisation was unaffected by coexpression of TSC2 (Figure 4H and I) or by MG-132 treatment (Figure 4K). The intracellular localisation patterns of the L61P, L93R, V133F and R190P variants were indistinguishable from the L50P variant (data not shown).

**Discussion**

We investigated the effects of 13 putative pathogenic amino acid substitutions on TSC1 function. Our findings are summarised in Table 1. The *TSC1* c.149T>C (p.L50P), c.182T>C (p.L61P), c.278T>G (p.L93R), c.397G>T (p.V133F) and c.569G>C (p.R190P) changes resulted in reduced levels of TSC1, a reduction in the TSC1-TSC2-dependent inhibition of mTOR activity and a distinct intracellular

expression pattern compared to wild-type TSC1. We conclude that these changes are pathogenic. According to the LOVD *TSC1* mutation database the p.L61P and p.L93R substitutions are probably pathogenic [18]. Our functional analysis supports this conclusion. The p.L50P, p.V133F and p.R190P substitutions are classified as being of unknown pathogenicity in the database. Our data indicates that these changes are pathogenic.

Several studies indicate that *TSC1* mutations are associated with a less severe clinical presentation in TSC patients [7 - 9] and further study is required to determine whether patients with a *TSC1* missense mutation follow this pattern, or have a distinct phenotypic spectrum compared to other TSC patient groups.

The c.153A>C (p.E51D), c.568C>T (p.R190C), c.1001C>T (p.S334L), c.1648C>G (p.Q550E), c.1974C>G (p.D658E), c.1976C>T (p.A659V) and c.2420T>C (p.I807T) substitutions did not affect TSC1 in our assays and were predicted to have no effect on *TSC1* mRNA splicing. The LOVD *TSC1* mutation database lists the c.153A>C (p.E51D), c.568C>T (p.R190C) and c.1001C>T (p.S334L) variants as probably not pathogenic, and our functional analysis indicates that they are neutral variants. Furthermore, mutation screening in additional individuals with TSC resulted in the identification of definite pathogenic *TSC2* mutations in patients carrying the c.153A>C (p.E51D), c.568C>T (p.R190C) and c.1001C>T (p.S334L) substitutions, confirming the classification of these variants as non-pathogenic (data not shown). The LOVD *TSC1* mutation database lists the c.1648C>G (p.Q550E) and c.2420T>C (p.I807T) variants as being of unknown pathogenicity. Our analysis indicates that these variants are not pathogenic, although we could not confirm experimentally that they do not affect *TSC1* mRNA splicing.

The c.1433A>G (E478G) substitution is listed as being of unknown pathogenicity and did not affect TSC1 function in our assays. However, one of three splice site prediction programs identified a potential effect of this substitution on splicing. We did not have access to RNA from this particular individual so we compared the activity of the protein product of the predicted splice isoform to wild-type TSC1, the E478G variant and the L117P pathogenic variant. We did not observe any differences between the predicted TSC1 E478GinsGN variant and either wild-type TSC1 or the E478G (Supplemental Figure 1). Therefore, we did not find any evidence that the c.1433A>G substitution was pathogenic.

All of the amino acid substitutions that affected TSC1 function in our assays were in the N-terminal region of TSC1 and were shown by our SIFT analysis to be relatively intolerant of amino acid changes (amino acids 1 - 270; see Figure 1). Two amino acid substitutions from this region, p.E51D and p.R190C, did not affect TSC1 function in our assays. Aspartate (E) and glutamate (D) are acidic amino acids. The BLOSUM 62 and Grantham matrices classify this substitution as conservative (Figure 1A and B) and our SIFT analysis predicted that the p.E51D substitution should be tolerated (Table 1). Therefore, in this case, the experimental data were in agreement with the *in silico* predictions. In contrast, the p.R190C substitution was non-conservative according to the BLOSUM 62 and Grantham matrices and was not tolerated according to our SIFT analysis. The predictions were therefore inaccurate for this particular amino acid substitution since the functional analysis did not reveal an effect on TSC1 function, and genetic analysis indicated that the substitution was not pathogenic. This result demonstrates that a conclusion with respect to pathogenicity based on *in silico* analysis only should be made with caution.

To provide clinicians and researchers with the maximum amount of information, gene variant databases should move towards incorporating both *in vitro* and *in silico* data [32]. We will add the functional and *in silico* results on the variants described here to the LOVD *TSC1* database as part of the individual entries. We will include the BLOSUM 62, Grantham and SIFT scores as well as the potential splice effects of the different variants. However, for all apparent missense variants, conclusions with regard to pathogenicity will continue to rely on clinical, family and functional data. As the above example shows, although *in silico* analysis is a valuable research tool, it is not yet reliable enough to inform clinical decisions.

One explanation for the apparent clustering of pathogenic amino acid substitutions to the N-terminal region is that this region is critical for TSC1 function. Alternatively, the pathogenic amino acid substitutions may simply be less conservative than the neutral variants we tested. Although the pathogenic substitutions in the TSC1 N-terminal region were not conservative, there was no clear distinction between these changes and other neutral substitutions. For example, as shown in Figure 1, the neutral p.R190C variant is a non-conservative, non-tolerated substitution that is predicted to have a large effect on TSC1 hydrophobicity, while the pathogenic p.R190P variant is a more conservative substitution and has a less dramatic effect on TSC1 hydrophobicity. Similarly, the p.V133F substitution is more conservative than the p.R190C substitution and has a relatively mild effect on TSC1 hydrophobicity, yet still has a dramatic effect on TSC1 function in our assays. In addition to the p.E51D and p.R190C substitutions, 6 other TSC1 amino acid substitutions did not affect TSC1 function in our assays. The neutral p.S334L and p.E478G substitutions are non-conservative changes located within the substitution-tolerant central region of TSC1 defined by the SIFT analysis (amino acids 270 - 680; see Figure 1). The neutral, non-conservative p.I807T substitution lies

outside this central region, but was also predicted by the SIFT algorithm to be tolerated (Table 1). The neutral p.Q550E, p.A659V and p.D658E substitutions are all conservative, tolerated changes. The results of the *in silico* and functional analyses are consistent with the N-terminal of TSC1 being a conserved, substitution-intolerant region of the protein that has an important role in maintaining TSC1 expression and activity in the cell.

The L50P, L61P, L93R, V133F and R190P variants were detected at lower levels compared to wild-type TSC1 and the E51D, R190C, S334L, Q550E, D658E, A659V and I807T variants. Inhibition of proteosome-mediated degradation resulted in increased levels of the L50P and L117P variants, indicating that the pathogenic TSC1 variants are normally rapidly degraded by the proteosome. Interestingly, increasing the levels of the TSC1 L50P and L117P variants by inhibiting proteosome activity resulted in an increase in mTOR activity, as estimated by the extent of S6K T389 phosphorylation. Therefore, increased expression of the L50P and L117P variants had a dominant negative effect on mTOR signalling. One possible explanation for this effect is that the mutant variants sequester TSC2 in inactive TSC1-TSC2 complexes, thereby reducing the capacity of the cells to inhibit mTOR activity. Therefore, MG-132 treatment may help distinguish more clearly between pathogenic and non-pathogenic TSC1 variants.

It is unlikely that this dominant negative effect is significant *in vivo* in TSC patients because, as our studies indicate, the L50P and L117P variants are rapidly degraded compared to wild-type TSC1 (Figure 2A). However, it could provide an explanation for the relative scarcity of *TSC1* missense mutations. It is possible that other missense variants are stable and do have a dominant negative effect on TSC1-TSC2 function *in vivo* that is incompatible with embryonic survival.

Further study is required to explore in more detail how the N-terminal region is important for TSC1 function. One possibility is that it is necessary for the proposed membrane localisation of TSC1 [33]. Alternatively, it may mediate other inter- or intramolecular interactions. Our observation that pathogenic amino acid substitutions prevent the formation of large TSC1-containing aggregate structures suggests that the N-terminal domain may mediate TSC1 homodimerisation.

## Conclusion

We have analysed 13 *TSC1* variants identified in TSC patients that cause missense changes to the TSC1 protein, and identified 5 pathogenic substitutions. Our data confirm that functional assays can be used to differentiate between neutral and pathogenic variants, facilitating the identification of pathogenic mutations in individuals with TSC and providing insight into how specific amino acid residues contribute to protein function.

The N-terminal region of TSC1 (amino acids 1 - 270) is essential for TSC1 function. Amino acid changes to this region prevent the formation of large TSC1 aggregates and promote proteosome-mediated degradation of the protein, thereby reducing steady state levels of TSC1 and resulting in increased signalling through mTOR. Rapid degradation of the mutant TSC1 isoforms *in vivo* most likely prevents the possible dominant negative effects of these variants on TSC1-TSC2-dependent inhibition of mTOR signalling.

## Abbreviations

TSC, tuberous sclerosis complex; GAP, GTPase activating protein; mTOR, mammalian target of rapamycin; S6K, p70 S6 kinase.

## Competing interests

The authors declare that they have no competing interests.

## Authors' contributions

MM, MH-W and MN performed the practical work; mutation information was provided by DK, JS, AvdO and DH; RE, SP and JdD are responsible for curation of the LOVD *TSC1* mutation database. The manuscript was drafted by MN and read and approved by all authors.

## Acknowledgments

Financial support was provided by the U.S. Department of Defense Congressionally-Directed Medical Research Program (grant #TS060052), NIH NINDS NS31535 and the Tuberous Sclerosis Alliance. The authors report no conflicts of interest.

## References

1. Gomez M, Sampson J, Whittemore V, eds. *The tuberous sclerosis complex*. Oxford, UK: Oxford University Press; 1999.

2. Roach ES, DiMario FJ, Kandt RS: **Tuberous sclerosis consensus conference: recommendations for diagnostic evaluation. National Tuberous Sclerosis Association.** *J Child Neurol* 1999, **14**:401-407.

3. van Slegtenhorst M, de Hoogt R, Hermans C: **Identification of the tuberous sclerosis gene *TSC1* on chromosome 9q34.** *Science* 1997, **277**:805-808.

4. The European Chromosome 16 Tuberous Sclerosis Consortium: **Identification and characterization of the tuberous sclerosis gene on chromosome 16.** *Cell* 1993, **75**:1305-1315.

5. Jones AC, Shyamsundar MM, Thomas MW: **Comprehensive mutation analysis of *TSC1* and *TSC2*, and phenotypic correlations in 150 families with tuberous sclerosis.** *Am J Hum Genet* 1999, **64**:1305-1315.

6. Dabora SL, Jozwiak S, Franz DN: **Mutational analysis in a cohort of 224 tuberous sclerosis patients indicates increased severity of *TSC2*, compared with *TSC1*, disease in multiple organs.** *Am J Hum Genet* 2001, **68**:64-80.

7. Sancak O, Nellist M, Goedbloed M: **Mutational analysis of the *TSC1* and *TSC2* genes in a diagnostic setting: genotype-phenotype correlations and comparison of diagnostic DNA techniques in tuberous sclerosis complex.** *Eur J Hum Genet* 2005, **13**:731-741.

8. Niida Y, Lawrence-Smith N, Banwell A: **Analysis of both *TSC1* and *TSC2* for germline mutations in 126 unrelated patients with tuberous sclerosis.** *Hum Mutat* 1999, **14**:412-422.

9. Au K-S, Williams AT, Roach ES: **Genotype/phenotype correlation in 325 individuals referred for a diagnosis of tuberous sclerosis complex in the United States.** *Genet Med* 2007, **9**:88-100.

10. Nellist M, Sancak O, Goedbloed MA: **Distinct effects of single amino acid changes to tuberin on the function of the tuberin-hamartin complex.** *Eur J Hum Genet* 2005, **13**:59-68.

11. Nellist M, van den Heuvel D, Schluep D: **Missense mutations to the *TSC1* gene cause tuberous sclerosis complex.** *Eur J Hum Genet* 2009, **17**:301-310.

12. van Slegtenhorst M, Nellist M, Nagelkerken B: **Interaction between hamartin and tuberin, the *TSC1* and *TSC2* gene products.** *Hum Mol Genet* 1998, **7**:1053-1057.

13. Li Y, Corradetti MN, Inoki K: **TSC2: filling the GAP in the mTOR signaling pathway.** *Trends Biochem Sci* 2003, **28**:573-576.

14. Rosner M, Hanneder M, Siegel N: **The tuberous sclerosis gene products hamartin and tuberin are multifunctional proteins with a wide spectrum of interacting partners.** *Mut Res* 2008, **658**:234-246.

15. Huang J and Manning BD: **The TSC1-TSC2 complex: a molecular switchboard controlling cell growth.** *Biochem J* 2008, **412**:179-90.

16. Nellist M, Sancak O, Goedbloed MA: **Functional characterisation of the TSC1-TSC2 complex to assess multiple TSC2 variants identified in single families affected by tuberous sclerosis complex.** *BMC Med Genet* 2008, **9**:10.

17. Pymar LS, Platt FM, Askham JM: **Bladder tumour-derived somatic TSC1 missense mutations cause loss of function via distinct mechanisms.** *Hum Mol Genet* 2008, **17**:2006-2017.

18. Tuberous sclerosis database - Leiden Open Variation Database [www.LOVD.nl/TSC1].

19. Fokkema IF, den Dunnen JT and Taschner PE: **LOVD: easy creation of a locus-specific sequence variation database using an "LSDB-in-a-box" approach.** *Hum Mutat* 2005, **26**:63-68.

20. Henikoff S and Henikoff JG: **Amino acid substitution matrices from protein blocks.** *Proc Natl Acad Sci USA* 1992, **89**:10915-10919.

21. Grantham R: **Amino acid difference formula to help explain protein evolution.** *Science* 1973, **185**:862-864.

22. Ng PC and Henikoff S: **Predicting the effects of amino acid substitutions on protein function.** *Annu Rev Genomics Hum Genet* 2006, **7**:61-80.

23. Ng PC and Henikoff S: **Accounting for human polymorphisms predicted to affect protein function.** *Genome Res* 2002, **12**:436-446.

24. Adamczak R, Porollo A and Meller J: **Accurate Prediction of Solvent Accessibility Using Neural Networks Based Regression.** *Proteins: Structure, Function and Bioinformatics* 2004, **56**:753-767.

25. Jones DT: **Protein secondary structure prediction based on position-specific scoring matrices.** *J Mol Biol* 1999, **292**:195-202.

26. NetGene2 Server [www.cbs.dtu.dk/services/NetGene2].

27. BDGP: Splice Site Prediction by Neural Network [www.fruitfly.org/seq_tools/splice.html].

28. Human Splicing Finder [www.umd.be/HSF/HSF.html].

29. Coevoets R, Arican S, Hoogeveen-Westerveld M: **A reliable cell-based assay for testing unclassified *TSC2* gene variants.** *Eur J Hum Genet* 2009, **17**:319-328..

30. Lee DH and Goldberg AL: **Proteasome inhibitors: valuable new tools for cell biologists.** *Trends Cell Biol* 1998, **8**:397-403.

31. Nellist M, van Slegtenhorst MA, Goedbloed M: **Characterization of the cytosolic tuberin-hamartin complex: tuberin is a cytosolic chaperone for hamartin.** *J Biol Chem* 1999, **274**:35647-35652.

32. Cotton RG, Auerbach AD, Axton M: **Genetics. The Human Variome Project.** *Science* 2008, **322**:861-862

33. Cai SL, Tee AR, Short D: **Activity of TSC2 is inhibited by AKT-mediated phosphorylation and membrane partitioning.** *J Cell Biol* 2006, **173**:279-89.

**Table 1.**

| Nucleotide change | Exon | Amino acid substitution | SIFT prediction | Effect on TSC1 function? (t-test) | Conclusion |
|---|---|---|---|---|---|
| c.149T>C | 4 | p.L50P | not tolerated | yes (p = 0.03) | pathogenic |
| c.153A>C | 4 | p.E51D | tolerated | no (p = 0.3) | neutral variant |
| c.182T>C | 4 | p.L61P | not tolerated | yes (p = 0.002) | pathogenic |
| c.278T>G | 5 | p.L93R | not tolerated | yes (p = 0.03) | pathogenic |
| c.397G>T | 6 | p.V133F | not tolerated | yes (p = 0.005) | pathogenic |
| c.569G>C | 7 | p.R190P | not tolerated | yes (p = 0.004) | pathogenic |
| c.568C>T | 7 | p.R190C | not tolerated | no (p = 0.19) | neutral variant |
| c.1001C>T | 10 | p.S334L | tolerated | no (p = 0.19) | neutral variant |
| c.1433A>G | 14 | p.E478G | tolerated | no (p = 0.6) | possible splice mutation |
| c.1648C>G | 15 | p.Q550E | tolerated | no (p = 0.9) | neutral variant |
| c.1974C>G | 15 | p.D658E | tolerated | no (p = 0.13) | neutral variant |
| c.1976C>T | 15 | p.A659V | tolerated | no (p = 0.1) | neutral variant |

| | | | | | |
|---|---|---|---|---|---|
| c.2420T>C | 19 | p.I807T | tolerated | no (p = 0.18) | neutral variant |

**Titles and legends to figures**

**Figure 1:** Predicted effects of amino acid substitutions on TSC1.

(A) Plot of the BLOSUM 62 scores for amino acid substitutions listed in the LOVD *TSC1* mutation database. Amino acid substitutions investigated as part of this study are indicated. Positive values represent conservative substitutions, negative values represent non-conservative substitutions.

(B) Plot of the Grantham scores for amino acid substitutions listed in the LOVD *TSC1* mutation database. Amino acid substitutions investigated as part of this study are indicated. The higher the Grantham score, the less conservative the substitution.

(C) Results of the SIFT prediction analysis. Graphical representation of the SIFT analysis results for TSC1. Each amino acid is represented by a box. Solid green boxes represent positions that are completely tolerant (all amino acid changes are possible); open green boxes represent positions where one or two amino acid substitutions are not tolerated. Solid red boxes represent completely intolerant positions (no amino acid changes are tolerated); open red boxes represent positions where only three or fewer amino acid changes are tolerated. Empty boxes represent positions where between 3 and 17 substitutions are tolerated. These are the positions that do not fall into any of the other categories. The positions of the amino acid variants tested as part of this study are indicated in blue.

(D) and (E) Comparative hydrophobicity profiles of TSC1 and the TSC1 variants. Hydrophobicity values for each amino acid residue of wild-type and variant TSC1 isoforms were calculated using DNAMAN software (default parameters). The differences in the predicted hydrophobicity per amino acid residue between the wild-type and variant isoforms were plotted. Values > 0 indicate an increase in

hydrophobicity of the variant relative to the wild-type sequence; values < 0 indicate a decrease.

Variants predicted by the SIFT analysis to be tolerated are shown in the upper plot (D). The E51D, S334L, E478G, Q550E, D658E, A659V and I807T variants analysed as part of this study are indicated. The E51D, Q550E and D658E substitutions did not affect the TSC1 hydrophobicity profile. The relative positions of these substitutions are indicated with arrows.

Variants predicted by the SIFT analysis not to be tolerated are shown in the lower plot (E). The L50P, L61P, L93R, V133F, R190C and R190P variants analysed as part of this study are indicated.

**Figure 2:** Inhibition of S6K-T389 phosphorylation by TSC1 missense variants.
(A) Cells expressing S6K, TSC2 and wild-type TSC1 or the TSC1 variants were analysed by immunoblotting. Levels of TSC1, TSC2, total S6K and T389-phosphorylated S6K were determined using Odyssey$^{TM}$ near infra-red detection (Li-Cor Biosciences) and quantification software. As controls, cells transfected with expression constructs for wild-type TSC1 and S6K only (TSC1/S6K), TSC2 and S6K only (TSC2/S6K), S6K only (S6K) or empty vector only (control) were also analysed. S6K and the TSC1 variants were detected with an antibody specific for the myc epitope tag. The signals for the L117P, L50P, L61P, L93R, V133F and R190P single variants and L50P/I807T double variant were clearly reduced compared to wild-type TSC1 (see also B). Furthermore, S6K T389 phosphorylation was increased in the presence of the L117P, L50P, L61P, L93R, V133F, R190P and L50P/I807T variants compared to the E51D, R190C, S334L, E478G, Q550E, D658E, A659V and I807T variants. (see also D). A representative example of 3 separate experiments is shown.

(B) Quantification of the signals for the TSC1 variants detected by immunoblotting. The integrated intensities of the TSC1 signals for each variant were determined in 3 independent experiments. The TSC1 signals, relative to wild-type TSC1 (TSC1) were determined. Standard deviations are indicated. The signals for the L117P, L50P, L61P, L93R, V133F and R190P single variants and L50P/I807T double variant were significantly reduced compared to wild-type TSC1 and the E51D, R190C, S334L, E478G, Q550E, D658E, A659V and I807T variants (unpaired t-test, p values < 0.05, indicated with asterisks on the graph).

(C) Quantification of the signal for TSC2 detected in the presence of the TSC1 variants by immunoblotting. The integrated intensity of the TSC2 signal in the presence of each of the different TSC1 variants was determined in 3 independent experiments. The TSC2 signals, relative to the signal in the presence of wild-type TSC1 (TSC1), were determined. Standard deviations are indicated. The TSC2 signals in the presence of the different TSC1 variants were not significantly different from the TSC2 signal in the presence of wild-type TSC1 (unpaired t-test, p values >0.05).

(D) Inhibition of S6K T389 phosphorylation in the presence of different TSC1 variants. The ratio of the T389 S6K phosphorylation signal intensity to the total S6K signal intensity (T389/S6K) was measured in 3 independent experiments. The integrated intensity of each band was determined using the Odyssey scanning software and the mean T389/S6K ratios, relative to the wild-type TSC1 (wild-type TSC1 T389/S6K ratio = 1) were determined. Standard deviations are indicated. The S6K-T389 phosphorylation: total S6K ratio in the presence of the L117P, L50P, L61P, L93R, V133F and R190P single variants and L50P/I807T double variant was significantly increased compared to wild-type TSC1 (unpaired t-test p values < 0.05, indicated with asterisks on the graph; see Table 1.). In contrast the values for the E51D, R190C,

S334L, E478G, Q550E, D658E, A659V and I807T variants were not significantly different from wild-type TSC1 (unpaired t-test p values > 0.05; see Table 1.).
(E) Quantification of the S6K signals detected in the presence of the TSC1 variants by immunoblotting. The integrated intensity of the total S6K signal in the presence of each of the different TSC1 variants was determined in 3 independent experiments using the Odyssey scanning software. The S6K signals, relative to the signal in the presence of wild-type TSC1 (TSC1), were determined. Standard deviations are indicated. The total S6K signals in the presence of the different TSC1 variants were not significantly different to the S6K signal in the presence of wild-type TSC1 (unpaired t-test, p values >0.05), indicating that transfection efficiency, gel-loading and blot transfer were relatively constant across all samples.

**Figure 3.** Proteosome-mediated degradation of pathogenic TSC1 missense variants.
(A) Representative immunoblot showing levels of TSC2, wild-type TSC1 and the TSC1 L50P, L61P, L93R, V133F, R190P, L50P/I807T and L117P variants in transfected HEK 293T cells treated with 42 μM MG-132 for 4 hours, or left untreated. The blot was also incubated with an antibody against ubiquitin (Ub) to control for the effect of the MG-132 treatment. The levels of ubiquitinated proteins are increased in the treated lanes.
(B) Representative immunoblot showing levels of TSC2, TSC1 variants (L50P, L117P) and wild-type (TSC1), S6K and T389-phosphorylated S6K (T389) in transfected HEK 293T cells treated with 42 μM MG-132 and 200 nM insulin (+ insulin/MG-132), 42 μM MG-132 only (+ MG-132), 200 nM insulin only (+ insulin), or left untreated (basal).
(C) Quantification of the immunoblot experiments showing MG-132-dependent inhibition of proteosome-mediated degradation of the TSC1 L50P and L117P variants.

The mean integrated intensities (arbitrary units) of the signals for wild-type TSC1 (black), and the L50P (grey) and L117P (white) variants are shown. Inhibition of proteosome-mediated degradation with MG-132 resulted in a relative increase in the signals for the L50P and L117P variants compared to wild-type TSC1 in both insulin stimulated and unstimulated cells.

(D) Quantification of the immunoblot experiments showing increased mTOR activity after treating cells expressing the TSC1 L50P or L117P variants with the proteosome inhibitor MG-132. To estimate mTOR activity, the ratio of the integrated intensity of the signal for T389-phosphorylated S6K to the integrated intensity for the total S6K signal was determined (T389/S6K ratio). The mean T389/S6K ratios (arbitrary units) are shown for wild-type TSC1 (TSC1) and the L50P and L117P variants, after treatment with MG-132 only (MG-132), insulin only (+ insulin), both reagents (+ insulin/MG-132) or untreated (basal). Compared to MG-132-treated cells expressing wild-type TSC1, MG-132 treatment of cells expressing the L50P and L117P variants increased the T389/S6K ratio, indicating increased mTOR activity.

**Figure 4:** Intracellular localisation of TSC1 detected by immunofluorescence microscopy.

(A - B) Immunofluorescence microscopy was performed on HEK 293T cells expressing the TSC1 E51D variant. (A) Punctate cytoplasmic localisation of the E51D variant; (B) DAPI nuclear stain. White scale bar: 5 µm

(C - E) Immunofluorescence microscopy was performed on HEK 293T cells coexpressing TSC2 and the TSC1 E51D variant. (C) Diffuse cytoplasmic localisation of the E51D variant in the presence of TSC2; (D) Diffuse cytoplasmic localisation of TSC2; (E) DAPI nuclear stain. White scale bar: 5 µm

(F - G) Immunofluorescence microscopy was performed on HEK 293T cells expressing the TSC1 L50P variant. (F) Diffuse cytoplasmic localisation of the L50P variant; (G) DAPI nuclear stain. White scale bar: 5 µm

(H - J) Immunofluorescence microscopy was performed on HEK 293T cells coexpressing TSC2 and the TSC1 L50P variant. (H) Diffuse cytoplasmic localisation of the L50P variant in the presence of TSC2; (I) Diffuse cytoplasmic localisation of TSC2; (J) DAPI nuclear stain. White scale bar: 5 µm

(K - L) Immunofluorescence microscopy was performed on HEK 293T cells expressing the TSC1 L50P variant and treated with MG-132. (K) Diffuse cytoplasmic localisation of the L50P variant after MG-132 treatment; (L) DAPI nuclear stain. White scale bar: 5 µm

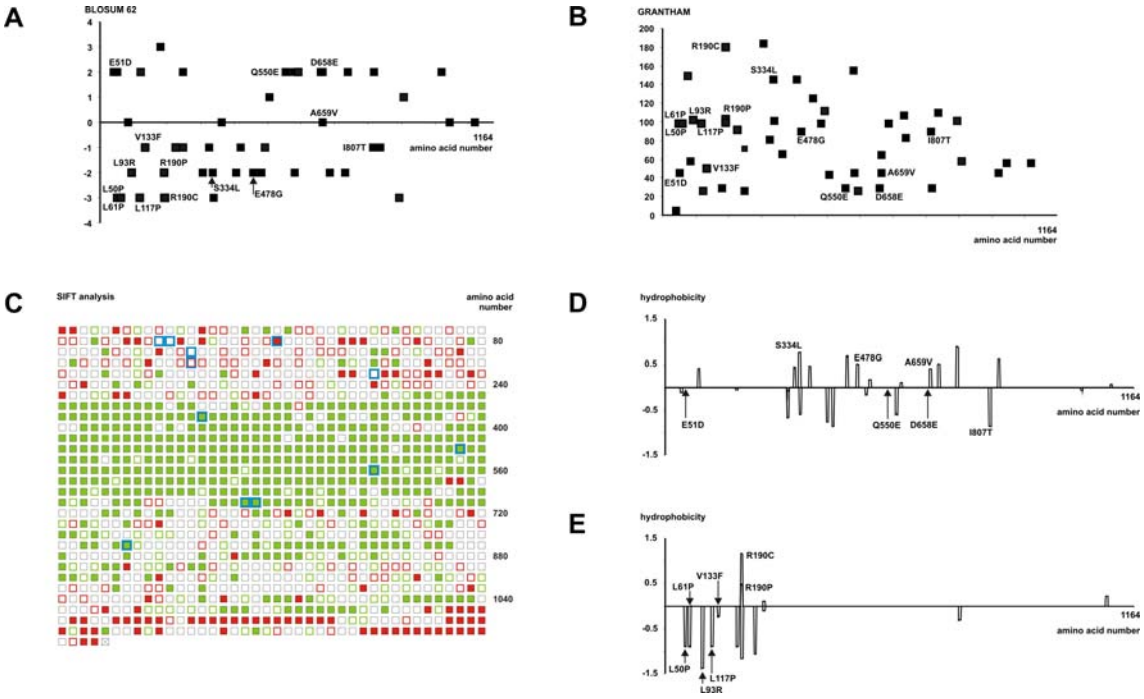

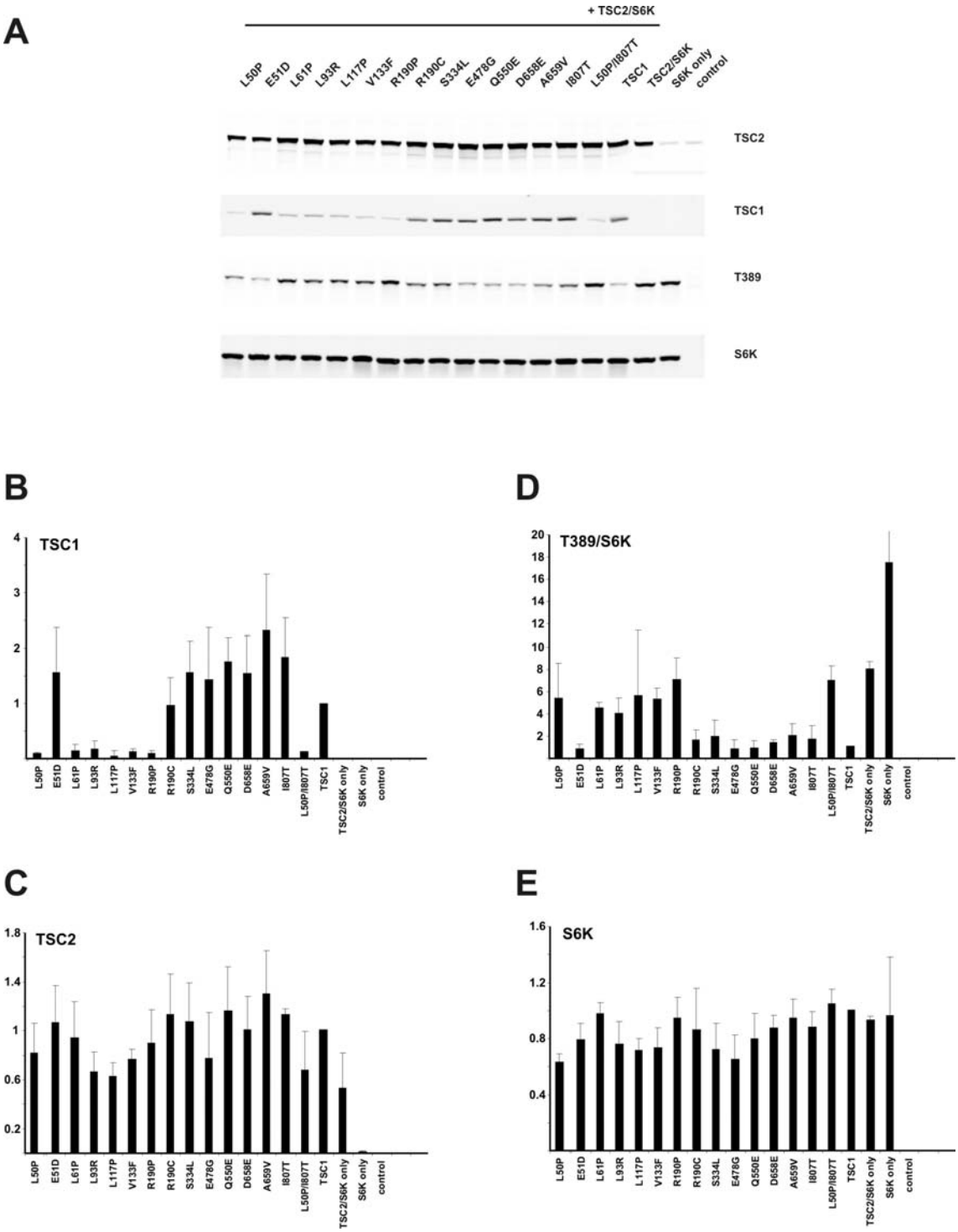
A
+ TSC2/S6K
L50P
E51D
L61P
L93R
L117P
V133F
R190P
R190C
S334L
E478G
Q550E
D658E
A659V
I807T
L50P/I807T
TSC1
TSC2/S6K
S6K only
control
TSC2
TSC1
T389
S6K
B
TSC1
C
TSC2
D
T389/S6K
E
S6K

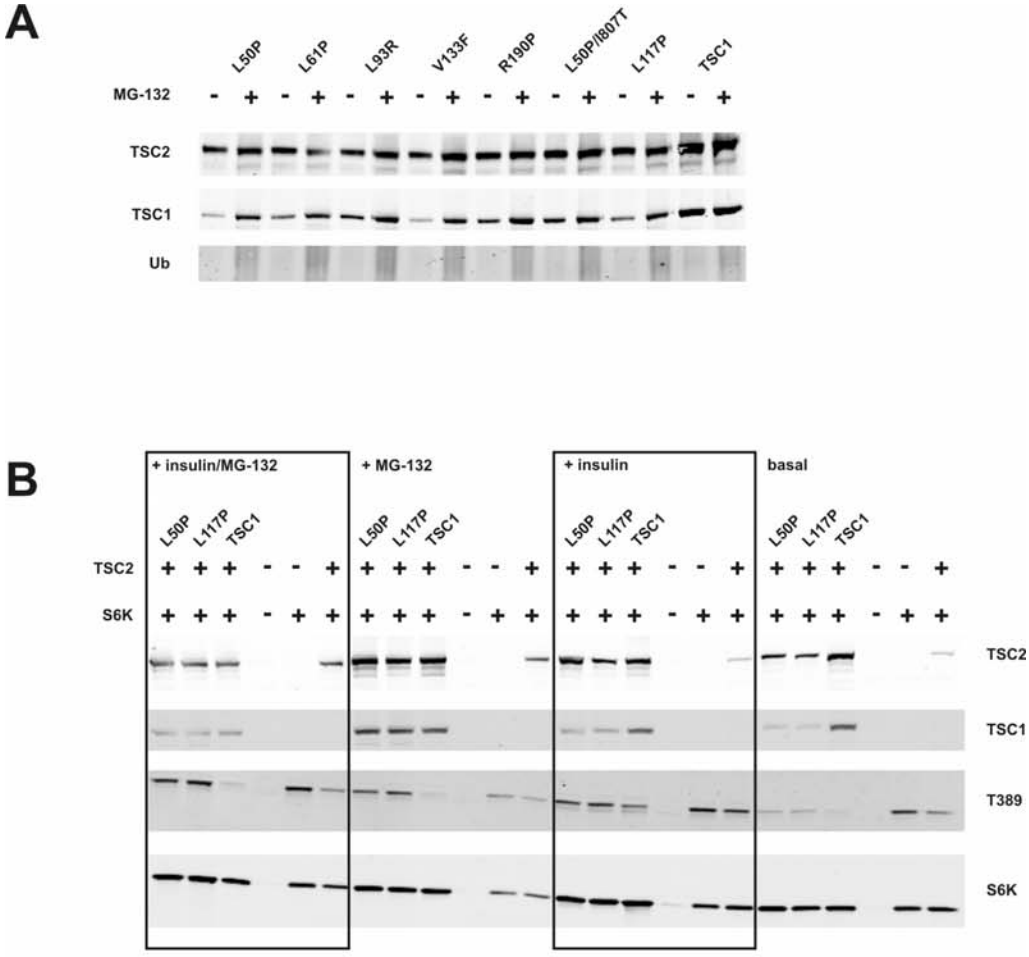
A
L50P
L61P
L93R
V133F
R190P
L50P/I807T
L117P
TSC1
MG-132
TSC2
TSC1
Ub
B
+ insulin/MG-132
+ MG-132
+ insulin
basal
L50P
L117P
TSC1
TSC2
S6K
TSC2
TSC1
T389
S6K
C
TSC1
TSC1
L50P
L117P
+ insulin/MG-132
+ MG-132
+ insulin
basal
D
T389/S6K
TSC1
L50P
L117P
+ insulin/MG-132
+ MG-132
+ insulin
basal

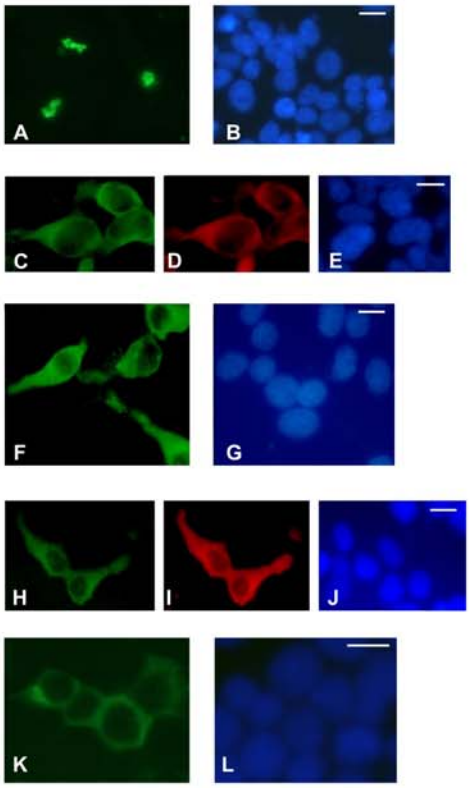
A
B
C
D
E
F
G
H
I
J
K
L

**Supplemental Figure:** Inhibition of S6K-T389 phosphorylation by the TSC1 E478GinsGN variant.

(A) Cells expressing S6K, TSC2 and wild-type TSC1 or the TSC1 L117P, E478G or E478GinsGN variants were analysed by immunoblotting. Levels of TSC1, TSC2, total S6K and T389-phosphorylated S6K were determined using Odyssey$^{TM}$ near infra-red detection (Li-Cor Biosciences) and quantification software. As controls, cells transfected with expression constructs for wild-type TSC1 and S6K only (TSC1/S6K), TSC2 and S6K only (TSC2/S6K), S6K only (S6K) or empty vector only (control) were also analysed. S6K and the TSC1 variants were detected with an antibody specific for the myc epitope tag. S6K T389 phosphorylation was reduced in the presence of wild-type TSC1 (TSC1) and the E478G variant compared to the L117P variant, consistent with Figure 2. The E478GinsGN variant reduced S6K-T389 phosphorylation as effectively as wild-type TSC1 and the E478G variant. A representative example of 3 separate experiments is shown.

(B) Quantification of the signal for the E478GinsGN variant as detected by immunoblotting. The signal for the E478GinsGN variant relative to wild-type TSC1 (TSC1) was determined in 3 independent experiments. The signal for the E478GinsGN variant was the same as wild-type TSC1 and the E478G variant. Standard deviations are indicated.

(C) Quantification of the signal for TSC2 detected in the presence of the E478GinsGN variant. The TSC2 signal in the presence of the E478GinsGN variant, relative to the signal in the presence of wild-type TSC1 (TSC1), was determined in 3 independent experiments. Standard deviations are indicated.

(D) Inhibition of S6K T389 phosphorylation in the presence of the E478GinsGN variant. The ratio of the S6K T389 phosphorylation signal intensity to the total S6K

signal intensity (T389/S6K) was measured in 3 independent experiments. The integrated intensity of each band was determined using the Odyssey scanning software and the mean T389/S6K ratios, relative to the wild-type TSC1 (wild-type TSC1 T389/S6K ratio = 1) were determined. Standard deviations are indicated. The S6K-T389 phosphorylation: total S6K ratio in the presence of the E478GinsGN variant was essentially the same as in the presence of wild-type TSC1.

(E) Quantification of the S6K signals detected in the presence of the TSC1 variants by immunoblotting. The integrated intensity of the total S6K signal in the presence of each of the different TSC1 variants was determined in 3 independent experiments using the Odyssey scanning software. The S6K signals, relative to the signal in the presence of wild-type TSC1 (TSC1), were determined. Standard deviations are indicated. The total S6K signals indicate that transfection efficiency, gel-loading and blot transfer were relatively constant across all samples.

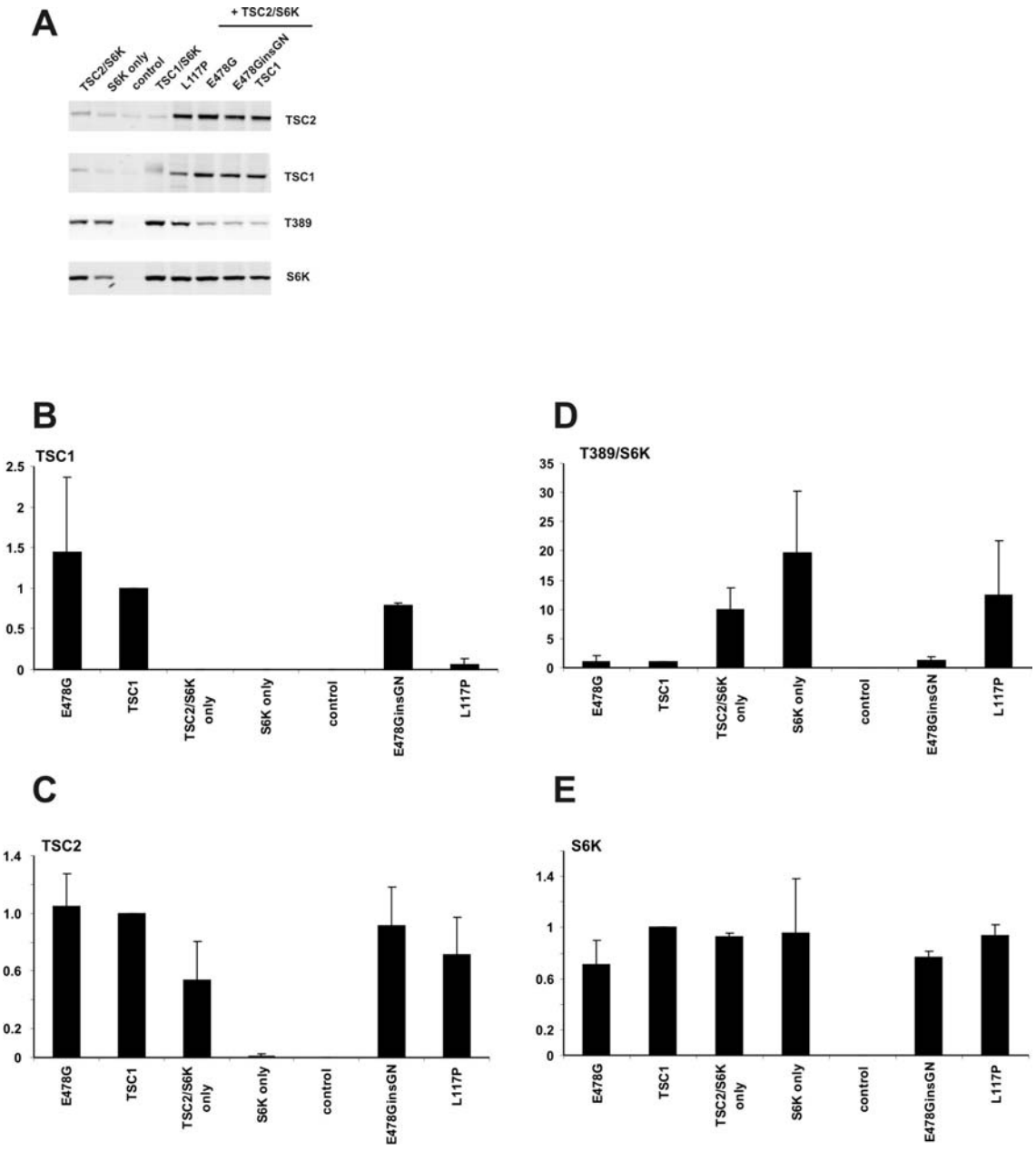
A
+ TSC2/S6K
TSC2/S6K
S6K only
control
TSC1/S6K
L117P
E478G
E478GinsGN
TSC1
TSC2
TSC1
T389
S6K
B
TSC1
2.5
2
1.5
1
0.5
0
E478G
TSC1
TSC2/S6K only
S6K only
control
E478GinsGN
L117P
D
T389/S6K
35
30
25
20
15
10
5
0
E478G
TSC1
TSC2/S6K only
S6K only
control
E478GinsGN
L117P
C
TSC2
1.4
1.0
0.6
0.2
0
E478G
TSC1
TSC2/S6K only
S6K only
control
E478GinsGN
L117P
E
S6K
1.4
1
0.6
0.2
0
E478G
TSC1
TSC2/S6K only
S6K only
control
E478GinsGN
L117P

**Supplemental Data Part 3. Figures.**

**Figure 1. Inhibition of S6K-T389 phosphorylation by TSC1 missense variants.**

(A) Cells expressing S6K, TSC2 and wild-type TSC1 or the TSC1 variants were analysed by immunoblotting. Levels of TSC1, TSC2, total S6K and T389-phosphorylated S6K were determined using Odyssey$^{TM}$ near infra-red detection (Li-Cor Biosciences) and quantification software. As controls, cells transfected with expression constructs for wild-type TSC1 and S6K only (TSC1/S6K), TSC2 and S6K only (TSC2/S6K), S6K only (S6K) or empty vector only (control) were also analysed. S6K and the TSC1 variants were detected with an antibody specific for the myc epitope tag. The signals for the L117P, L72P, I76N, L191R and L191H variants are clearly reduced compared to wild-type TSC1 (see also C). Furthermore, S6K T389 phosphorylation was increased in the presence of these variants (see also D). A representative example of 3 separate experiments is shown.

(B) Quantification of the signal for TSC2 detected in the presence of the TSC1 variants by immunoblotting. The integrated intensity of the TSC2 signal in the presence of each of the different TSC1 variants was determined in 3 independent experiments. The TSC2 signals, relative to the signal in the presence of wild-type TSC1 (TSC1), were determined. Standard deviations are indicated. The TSC2 signals in the presence of the different TSC1 variants were not significantly different from the TSC2 signal in the presence of wild-type TSC1 (unpaired t-test, p values >0.05), indicating that transfection efficiency, gel-loading and blot transfer were relatively constant across all samples.

(C) Quantification of the signals for the TSC1 variants detected by immunoblotting. The integrated intensities of the TSC1 signals for each variant were determined in 3 independent experiments. The TSC1 signals, relative to wild-type TSC1 (TSC1) were determined. Standard deviations are indicated.

(D) Inhibition of S6K T389 phosphorylation in the presence of different TSC1 variants. The ratio of the T389 S6K phosphorylation signal intensity to the total S6K signal intensity (T389/S6K) was measured in 3 independent experiments. The integrated intensity of each band was determined using the Odyssey scanning software and the mean T389/S6K ratios, relative to the wild-type TSC1 (wild-type TSC1 T389/S6K ratio = 1) were determined. Standard deviations are indicated.

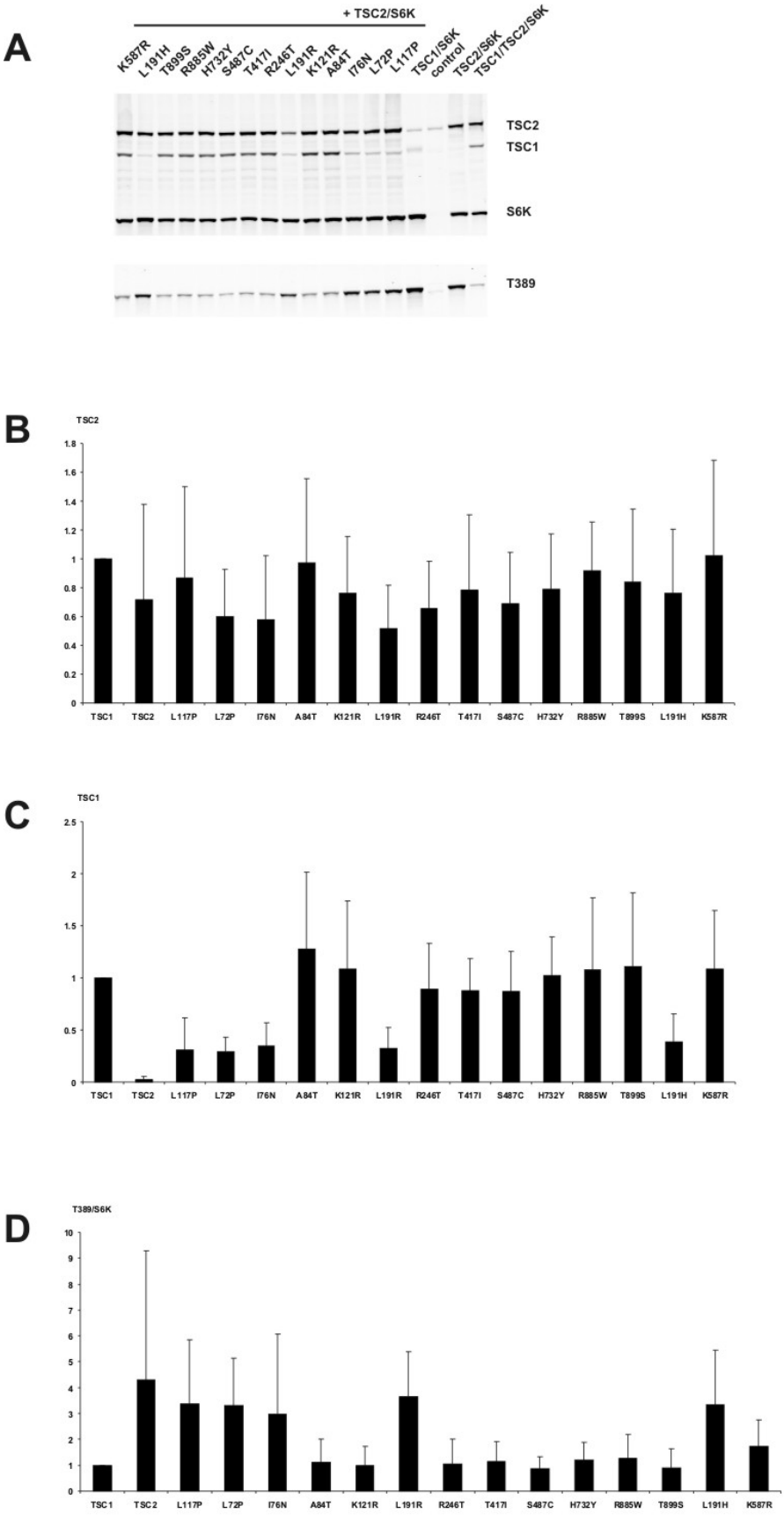
A
+ TSC2/S6K
K587R
L191H
T899S
R885W
H732Y
S487C
T417I
R246T
L191R
K121R
A84T
I76N
L72P
L117P
TSC1/S6K
control
TSC2/S6K
TSC1/TSC2/S6K
TSC2
TSC1
S6K
T389
B
TSC2
C
TSC1
D
T389/S6K
TSC1
TSC2
L117P
L72P
I76N
A84T
K121R
L191R
R246T
T417I
S487C
H732Y
R885W
T899S
L191H
K587R

**Figure 2. Inhibition of S6K-T389 phosphorylation by TSC2 missense variants.**

Cells expressing S6K, TSC1, and wild-type TSC2 or the TSC2 R611Q, R1200W, A889V, V334G, V334A or R57H variants were analysed by immunoblotting. Levels of TSC2, TSC1, total S6K and T389-phosphoprylated S6K were determined using Odyssey$^{TM}$ near infra-red detection (Li-Cor Biosciences) and quantification software. As controls, cells transfected with expression constructs for TSC1 and S6K only (TSC1/S6K), S6K only (S6K) or empty vector only (control) were also analysed.

(A) Representative immunoblot. S6K and TSC1 were detected with an antibody specific for the myc epitope tag. S6K-T389 phosphorylation was detected with a phospho-specific mouse monoclonal antibody (1A5, Cell Signaling Technology). TSC2 variants were detected with a rabbit polyclonal antibody raised against human TSC2 (11).

(B) Quantification of the signals for the TSC2 variants. The integrated intensities of the TSC2 signals were determined per lane. Standard deviations are indicated.

(C) Quantification of the signals for TSC1 in the presence of the different TSC2 variants. The integrated intensities of the TSC1 signals were determined per lane. Standard deviations are indicated. Note that the TSC1 signals in the presence of the R611Q, R57H, V334A, V334G and A889V variants are reduced compared to the signals in the presence of wild-type TSC2 or the R1200W variant.

(D) Inhibition of S6K T389 phosphorylation in the presence of the TSC2 variants. The integrated intensity of the T389-phosphorylated S6K and total S6K signals was determiend using the Odyssey scanning software and the ratio of the T389-phosphorylated S6K signal to the total S6K signal was calculated. Note that the T389/S6K ratio is clearly lower in the presence of wild-type TSC2, compared to all the other variants tested.

(E) Expression of S6K in the presence of the different TSC2 variants. The total S6K signals in the presence of the different TSC2 variants were approximately equal.

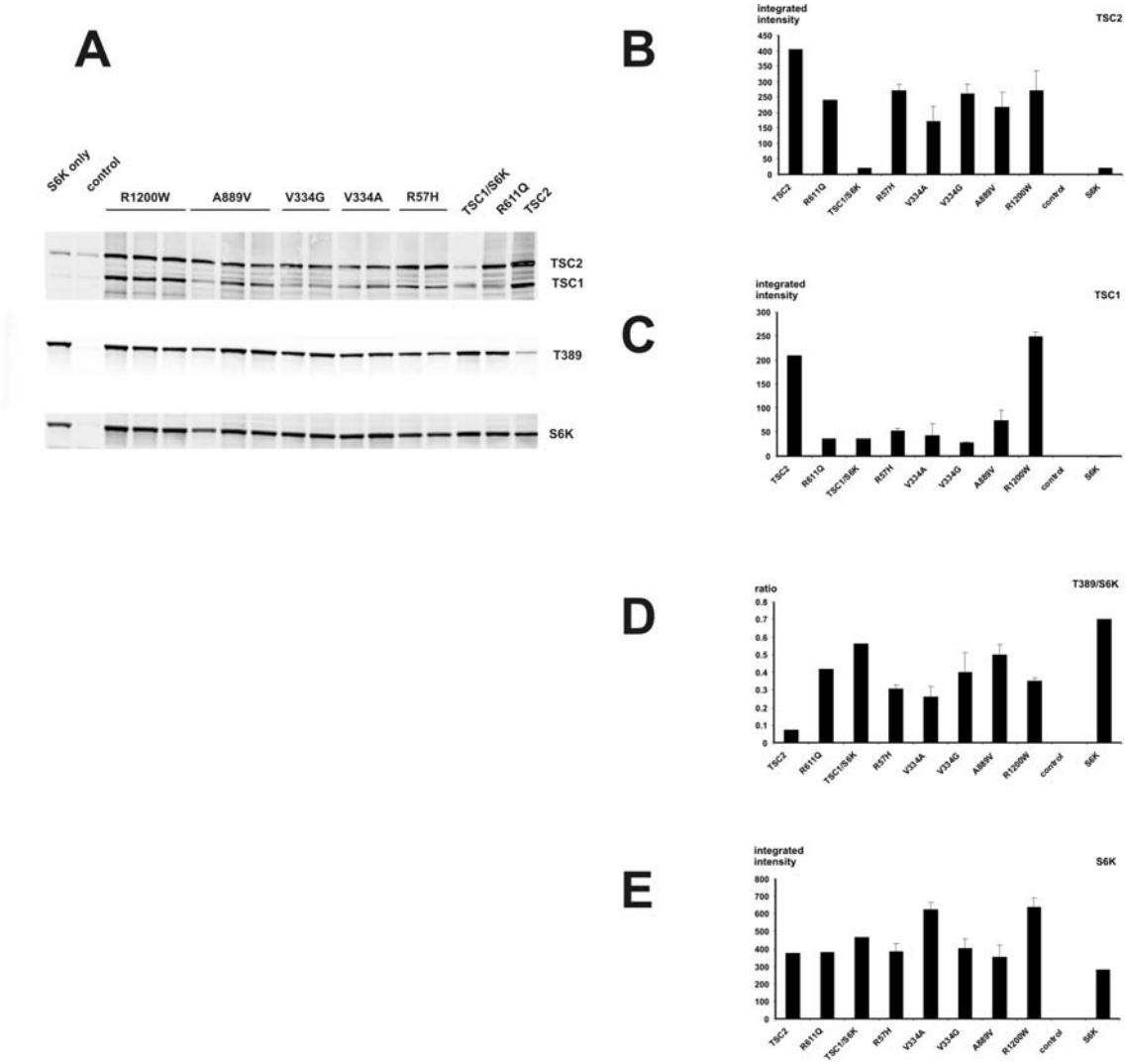
A
S6K only
control
R1200W
A889V
V334G
V334A
R57H
TSC1/S6K
R611Q
TSC2
TSC2
TSC1
T389
S6K
B
integrated intensity
TSC2
C
integrated intensity
TSC1
D
ratio
T389/S6K
E
integrated intensity
S6K
TSC2
R611Q
TSC1/S6K
R57H
V334A
V334G
A889V
R1200W
contrl
S6K

**Figure 3: Inhibition of S6K-T389 phosphorylation by TSC1 truncations.**

(A) Overview of TSC1 truncation constructs. The presence of the N- and C-termini are indicated, and the first and last amino acids are also indicated, where this differs from the full-length TSC1 protein (top). All cDNAs were cloned into a pcDNA3myc mammalian expression construct. Therefore, all proteins are expressed as fusion proteins with a C-terminal myc epitope tag. The TSC1 R509 truncation construct is not shown as it was tested in this assay. The TSC1 R509 truncation protein has the same molecular weight as S6K and therefore the 2 proteins could not be distinguished by immunoblotting.

(B) Cells expressing S6K, TSC2 and wild-type TSC1 (wt) or truncated TSC1 proteins were analysed by immunoblotting. TSC1, TSC2 and total S6K levels and levels of T389-phosphorylated S6K were determined Odyssey$^{TM}$ near infra-red detection and quantification software. As controls, cells transfected with expression constructs for wild-type TSC1 and S6K only (TSC1/S6K), TSC2 and S6K only (TSC2/S6K), S6K only (S6K) or empty vector only (control) were also analysed. S6K and the TSC1 truncations were detected with an antibody specific for the myc epitope tag. The signals for the TSC1 Q900 and M351 truncations were clearly reduced compared to wild-type TSC1 (see also Figure 5B). Furthermore, S6K T389 phosphorylation was increased in the presence of all the truncations compared to wild-type TSC1 (see also Figure 5C). A representative example of 3 separate experiments is shown.

(C) Expression of the TSC1 truncations. The integrated intensities of the TSC1 signals for each variant were determined in 3 independent experiments using the Odyssey scanning software. The TSC1 signals, relative to the wild-type TSC1 (TSC1 wt) were determined. Standard deviations are indicated.

(D) Expression of TSC2 in the presence of the TSC1 truncations. The integrated intensity of the TSC2 signal in the presence of each of the different TSC1 truncations was determined, relative to the signal in the presence of wild-type TSC1 (TSC1 wt). Standard deviations are indicated. The TSC2 signals in the presence of the different TSC1 variants were not significantly different to the TSC2 signal in the presence of wild-type TSC1 (unpaired t-test, p value >0.05).

(E) Inhibition of S6K T389 phosphorylation in the presence of different TSC1 truncations. The ratio of the T389 S6K phosphorylation signal intensity to the total S6K signal intensity (T389/S6K), relative to the wild-type TSC1 (wt) (wild-type TSC1

T389/S6K ratio = 1) was determined for each truncation. Standard deviations are indicated.

(F) Expression of S6K in the presence of the TSC1 truncations. The integrated intensity of the total S6K signal in the presence of each of the different TSC1 variants, relative to the signal in the presence of wild-type TSC1 (TSC1 wt), was determined for each truncation. Standard deviations are indicated. The total S6K signals in the presence of the different TSC1 variants were not significantly different to the S6K signal in the presence of wild-type TSC1 (unpaired t-test, p value >0.05), indicating that the transfection efficiency and gel-loading was relatively constant.

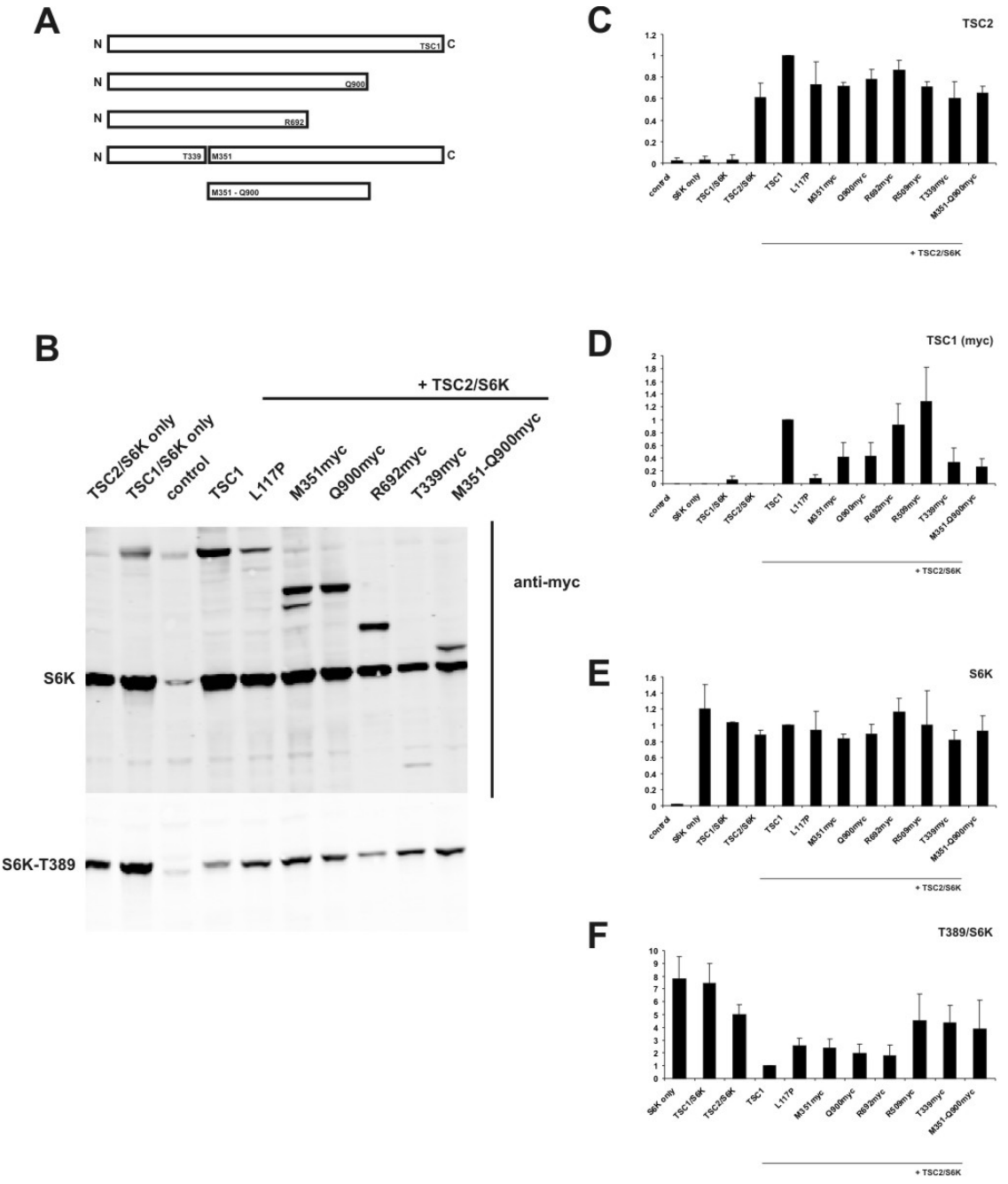
A
N
TSC1
C
N
Q900
N
R692
N
T339
M351
C
M351 - Q900
B
+ TSC2/S6K
TSC2/S6K only
TSC1/S6K only
control
TSC1
L117P
M351myc
Q900myc
R692myc
T339myc
M351-Q900myc
anti-myc
S6K
S6K-T389
C
TSC2
D
TSC1 (myc)
E
S6K
F
T389/S6K

**Figure 4. Schematic to show the putative effects of the *TSC2* c.1235A>T nucleotide change on the TSC2 amino acid sequence.**

The *TSC2* c.1235A>T nucleotide change is predicted to result in a E412V amino acid substitution. However, RT-PCR analysis of the patient RNA identified a novel splice isoform encoding a TSC2 variant lacking amino acids 413 - 420 (TSC2 412del8)

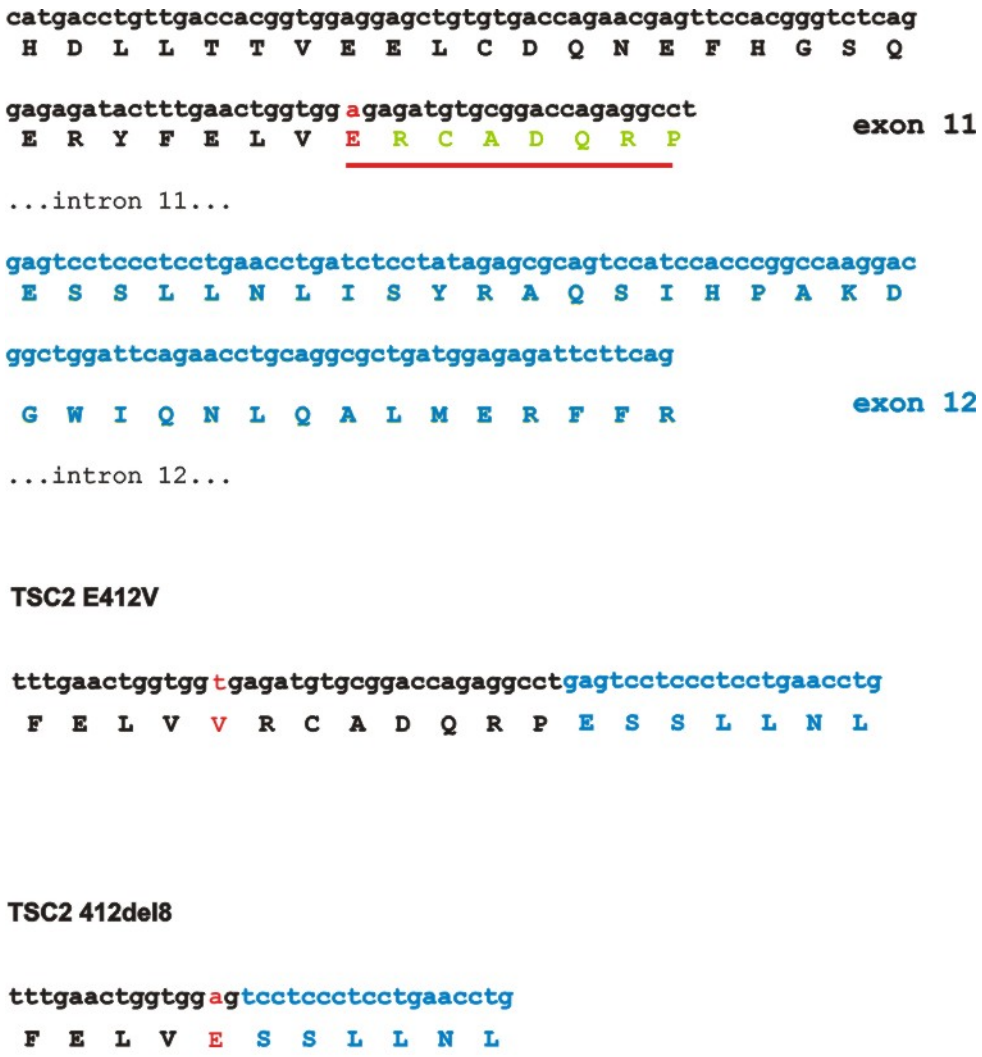

**Figure 5. Inhibition of S6K-T389 phosphorylation by a TSC2 splice variant.**

Cells expressing S6K, TSC1, and wild-type TSC2 or the TSC2 R611Q, E412V or 412del8 variants were analysed by immunoblotting. Levels of TSC2, TSC1, total S6K and T389-phosphoprylated S6K were determined using Odyssey$^{TM}$ near infra-red detection (Li-Cor Biosciences) and quantification software. As controls, cells transfected with expression constructs for TSC1 and S6K only (TSC1/S6K), S6K only (S6K) or empty vector only (control) were also analysed.

(A) Representative immunoblot. S6K and TSC1 were detected with an antibody specific for the myc epitope tag. S6K-T389 phosphorylation was detected with a phospho-specific mouse monoclonal antibody (1A5, Cell Signaling Technology). TSC2 variants were detected with a rabbit polyclonal antibody raised against human TSC2 (11).

(B) Quantification of the signals for the TSC2 variants. The integrated intensities of the TSC2 signals were determined per lane. Standard deviations are indicated.

(C) Quantification of the signals for TSC1 in the presence of the different TSC2 variants. The integrated intensities of the TSC1 signals were determined per lane. Standard deviations are indicated. Note that the TSC1 signals in the presence of the R611Q and 412del8 variants are reduced compared to the signals in the presence of wild-type TSC2 or the E412V variant.

(D) Inhibition of S6K T389 phosphorylation in the presence of the TSC2 variants. The integrated intensity of the T389-phosphorylated S6K and total S6K signals was determiend using the Odyssey scanning software and the ratio of the T389-phosphorylated S6K signal to the total S6K signal was calculated. Note that the T389/S6K ratio is clearly lower in the presence of wild-type TSC2 or the E412V variant compared to the R611Q or 412del8 variants.

(E) Expression of S6K in the presence of the different TSC2 variants. The total S6K signals in the presence of the different TSC2 variants were approximately equal.

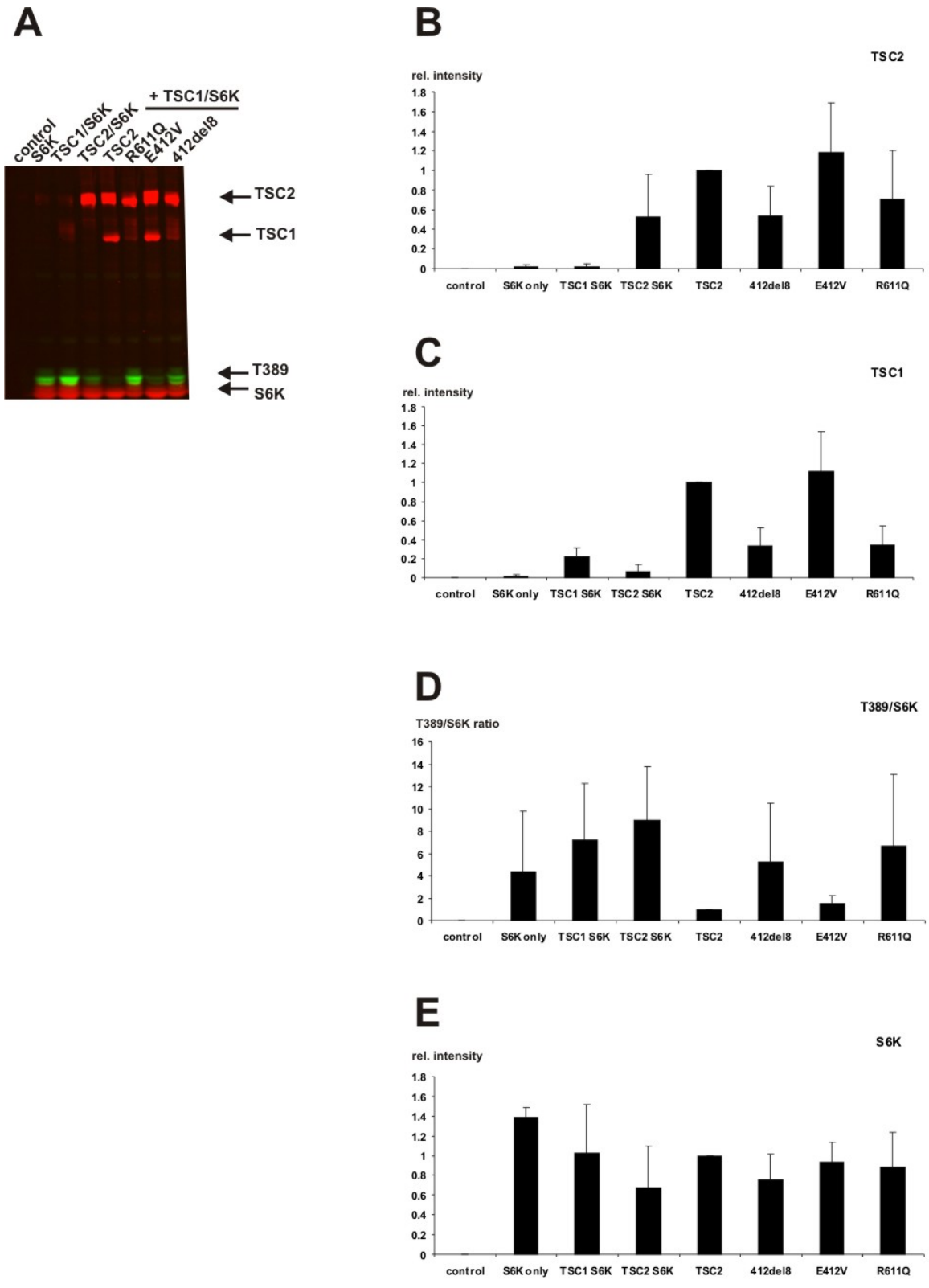
A
control
S6K
TSC1/S6K
TSC2/S6K
+ TSC1/S6K
TSC2
R611Q
E412V
412del8
TSC2
TSC1
T389
S6K
B
TSC2
rel. intensity
1.8
1.6
1.4
1.2
1
0.8
0.6
0.4
0.2
0
control
S6K only
TSC1 S6K
TSC2 S6K
TSC2
412del8
E412V
R611Q
C
TSC1
rel. intensity
1.8
1.6
1.4
1.2
1
0.8
0.6
0.4
0.2
0
control
S6K only
TSC1 S6K
TSC2 S6K
TSC2
412del8
E412V
R611Q
D
T389/S6K
T389/S6K ratio
16
14
12
10
8
6
4
2
0
control
S6K only
TSC1 S6K
TSC2 S6K
TSC2
412del8
E412V
R611Q
E
S6K
rel. intensity
1.8
1.6
1.4
1.2
1
0.8
0.6
0.4
0.2
0
control
S6K only
TSC1 S6K
TSC2 S6K
TSC2
412del8
E412V
R611Q

**Figure 6. Grantham scores for TSC2 amino acid substitutions identified in the Rotterdam TSC patient cohort**

(A) Grantham scores for confirmed pathogenic TSC2 amino acid substitutions identified in the Rotterdam TSC patient cohort. Amino acid number is plotted on the y-axis. Note that no pathogenic variants are present around amino acids 1200 - 1400.

(B) Grantham scores for all the TSC2 amino acid substitutions (pathogenic, neutral polymorphisms and unclassified variants) identiufied in the Rotterdam TSC patient cohort. Amino acid number is plotted on the y-axis.

**A**

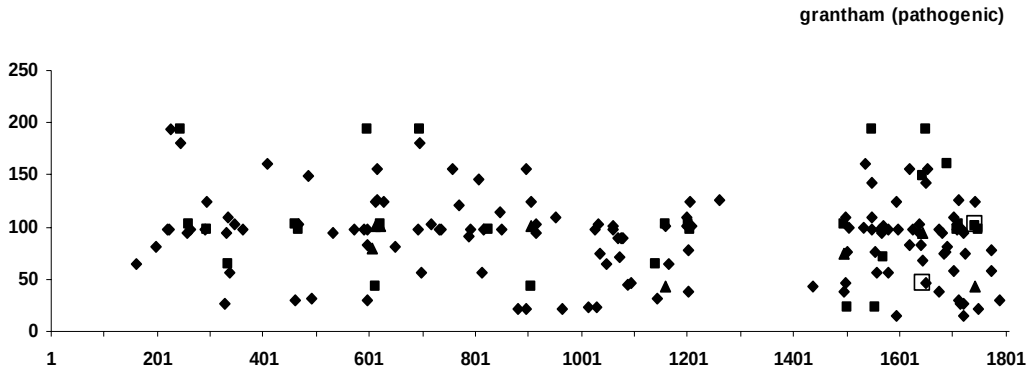


**B**

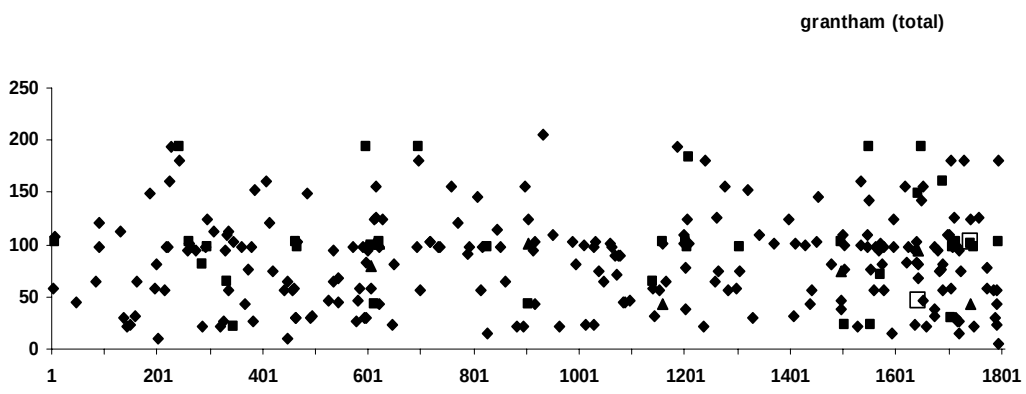

**Figure 7. SIFT prediction analysis of TSC1 and TSC2.**

(A) TSC1 SIFT prediction analysis. Graphical representation of the SIFT analysis results for TSC1. Each amino acid is represented by a box. Solid green boxes represent positions that are completely tolerant (all amino acid changes are possible); open green boxes represent positions where one or two amino acid substitutions are not tolerated. Solid red boxes represent completely intolerant positions (no amino acid changes tolerated); open red boxes represent positions where only three or fewer amino acid changes are tolerated. The stop codon is indicated in blue.

(B) TSC2 SIFT prediction analysis. Graphical representation of the SIFT analysis results for TSC2. Each amino acid is represented by a box. Solid green boxes represent positions that are completely tolerant (all amino acid changes are possible); open green boxes represent positions where one or two amino acid substitutions are not tolerated. Solid red boxes represent completely intolerant positions (no amino acid changes tolerated); open red boxes represent positions where only three or fewer amino acid changes are tolerated. The stop codon is indicated in blue.

# A

**TSC1 SIFT analysis**

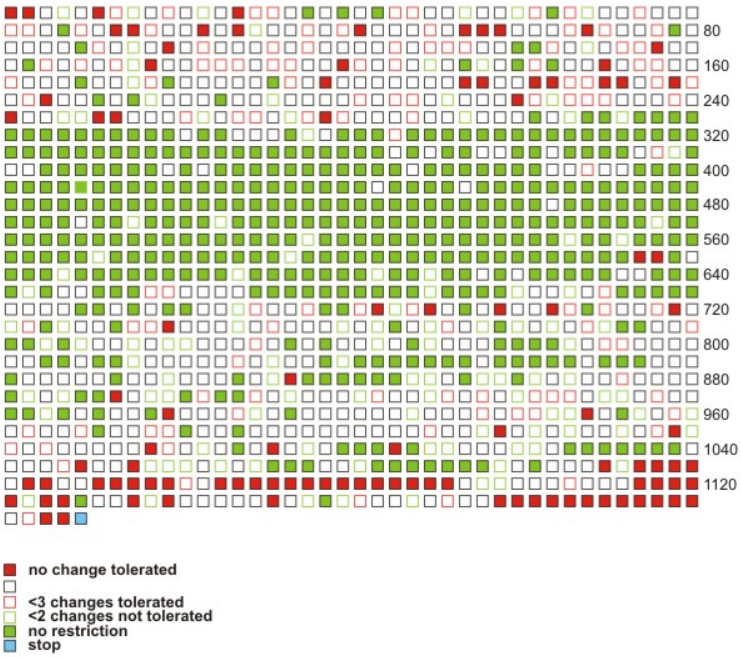


# B

**TSC2 SIFT analysis**

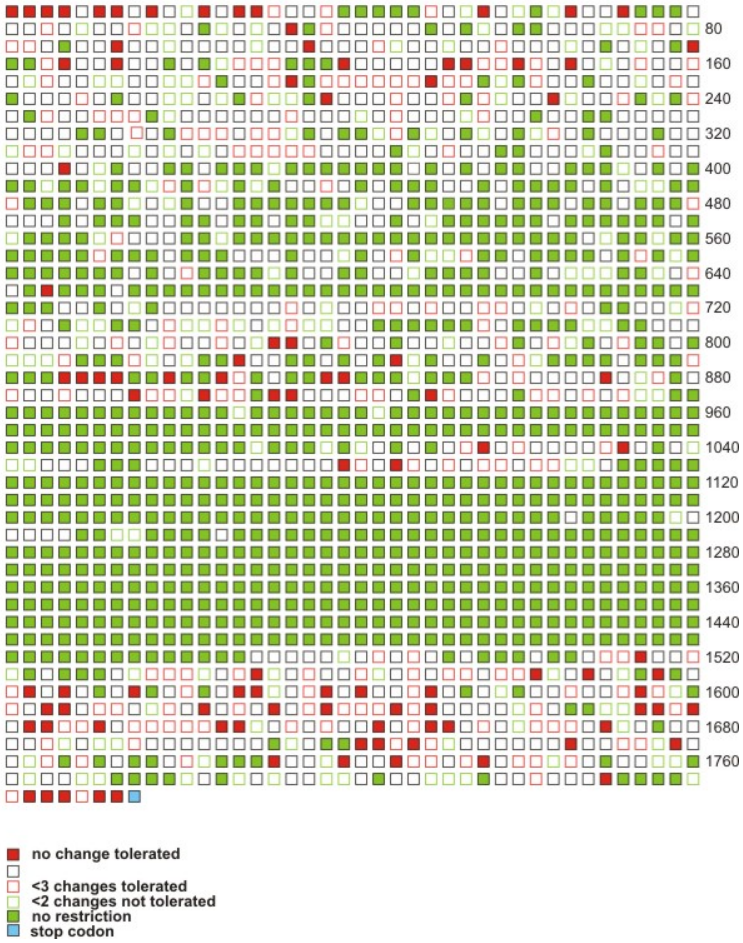

**Figure 8. Relative expression of TSC1 in the presence of different pathogenic TSC2 mutants, as detected by immunoblotting.**

(A) Quantification of the signals for the TSC2 variants. The mean integrated intensity of the TSC2 signals, relative to wild-type TSC2, were determined using the Odyssey near infra-red scanner (Li-Cor Biosciences). Signals from at least 3 independent experiments were determined for each variant. Standard deviations are indicated.

(B) Quantification of the signal for TSC1 in the presence of the different TSC2 variants. The mean integrated intensity of the TSC1 signals were determined, relative to the signal in the presence of wild-type TSC2, as in (A) above. The detected TSC1 signal is reduced in the presence of the TSC2 variants containing an amino acid change within the N-terminal 1000 amino acids.